



Aleppo pine seeds (*Pinus halepensis* Mill.) as a promising novel green coagulant for the removal of Congo red dye: Optimization via machine learning algorithm

Amina Hadadi, Ali Imessaoudene, Jean-Claude Bollinger, Abdelkrim Bouzaza, Abdeltif Amrane, Hichem Tahraoui, Lotfi Mouni

► To cite this version:

Amina Hadadi, Ali Imessaoudene, Jean-Claude Bollinger, Abdelkrim Bouzaza, Abdeltif Amrane, et al.. Aleppo pine seeds (*Pinus halepensis* Mill.) as a promising novel green coagulant for the removal of Congo red dye: Optimization via machine learning algorithm. *Journal of Environmental Management*, 2023, 331, pp.117286. 10.1016/j.jenvman.2023.117286 . hal-03971845

HAL Id: hal-03971845

<https://hal.science/hal-03971845>

Submitted on 31 Mar 2023

HAL is a multi-disciplinary open access archive for the deposit and dissemination of scientific research documents, whether they are published or not. The documents may come from teaching and research institutions in France or abroad, or from public or private research centers.

L'archive ouverte pluridisciplinaire **HAL**, est destinée au dépôt et à la diffusion de documents scientifiques de niveau recherche, publiés ou non, émanant des établissements d'enseignement et de recherche français ou étrangers, des laboratoires publics ou privés.

Aleppo pine seeds (*Pinus halepensis* Mill.) as a promising novel green coagulant for the removal of Congo red dye: optimization via machine learning algorithm

Amina Hadadi*¹, Ali Imessaoudene¹, Jean-Claude Bollinger², Abdelkrim Bouzaza³,
Abdeltif Amrane³, Hichem Tahraoui⁴, Lotfi Mouni¹

¹Laboratoire de Gestion et Valorisation des Ressources Naturelles et Assurance
Qualité. Faculté SNVST, Université de Bouira, 10000 Bouira, Algeria ;
a.imessaoudene@univ-bouira.dz (A.I.) ; l.mouni@univ-bouira.dz (L.M.)

²Laboratoire E2Lim, Université de Limoges, 123 Avenue Albert Thomas, 87060
Limoges, France ; jean-claude.bollinger@unilim.fr (J-C.B.)

³Univ.Rennes, ENSCR, 11 Allée de Beaulieu, 35708 Rennes, France ;
abdelkrim.bouzaza@ensc-rennes.fr (A.B.) abdeltif.amrane@univ-rennes1.fr (A.A.)

⁴Pharmaceutical Engineering Department, Process Engineering Faculty, Salah
Boubnider Constantine 3 University, Constantine, Algeria;
hichemm.tahraoui@gmail.com (H.T.)

* Correspondence: a.hadadi@univ-bouira.dz +213-561-456591.

Abstract

Consideration is now being given to the use of metal coagulants to remove turbidity from drinking water and wastewater. Concerns about the long-term impact of non-biodegradable sludge on human health and the potential contamination of aquatic systems are gaining popularity. Recently, alternative biocoagulants have been suggested to address these concerns. In this study, using a 1 M sodium chloride (NaCl) solution, the active coagulating agent was extracted from *Pinus halepensis* Mill. seed, and used for the first time to remove Congo red dye, the influence of numerous factors on dye removal was evaluated in order to make comparisons with conventional coagulants. The application of biocoagulant was shown to be very successful, with coagulant dosages ranging from 3 to 12 mL L⁻¹ achieving up to 80% dye removal and yielding 28 mL L⁻¹ of sludge. It was also found that biocoagulant is extremely pH sensitive with an optimum operating pH of 3. Ferric chloride, on the other hand, achieved similar removal rate with higher sludge production (46 mL L⁻¹) under the same conditions. A Fourier Transform Infrared Spectroscopy and proximate composition analysis were undertaken to determine qualitatively the potential active coagulant ingredient in the seeds and suggested the involvement of proteins in the coagulation-flocculation mechanism. The evaluation criteria of the Support vector machine_Gray wolf optimizer model in terms of statistical coefficients and errors reveals quite interesting results and demonstrates the performance of the model, with statistical coefficients close to 1 ($R = 0.9998$, $R^2 = 0.9995$ and $R^2_{adj} = 0.9995$) and minimal statistical errors (RMSE = 0.5813, MSE = 0.3379, EPM = 0.9808, ESP = 0.9677 and MAE = 0.2382).

The study findings demonstrate that *Pinus halepensis* Mill. seed extract might be a novel, environmentally friendly, and easily available coagulant for water and wastewater treatment.

Keywords: *Pinus halepensis* Mill. seed extract; biocoagulant; Congo red; coagulation-flocculation mechanism; Support Vector Machine, Gray Wolf Optimizer.

67 1. Introduction

68 Synthetic dyes are a significant class of recalcitrant organic compounds that are
69 frequently found in the environment because of their widespread use in several
70 industries; they are considered the most polluting of all industrial sectors. Dye
71 wastewater discharged onto surface waters such as rivers and lakes lowers light
72 transmission in the water, resulting in the reduction of photosynthesis as well as the
73 quantity of dissolved oxygen. Several researches stated that certain colors may
74 degrade and generate carcinogenic aromatic amines that are believed to remain in the
75 environment for a very long period (Momeni et al., 2018). As a result, there is an
76 unavoidable requirement for a dye/color removal method that is both successful and
77 cost-effective under the aforementioned circumstances (Crini et al., 2019; Mouni et al.,
78 2018).

79 Azo dyes are compounds with one or more azo linkages consisting of a
80 diazotized amine linked to an amine or phenol. The principal precursors of azo dyes
81 are aromatic amines. Almost two-thirds of all synthetic dyes are azo compounds.
82 Indeed, they are the most widely used and structurally diverse class of organic dyes
83 on the market owing to the vivid colors they exhibit (Ali et al., 2022). Azo dyes are also
84 stable to light and resistant to microbial degradation or discoloration caused by
85 washing. Therefore, it is difficult to remove these compounds from wastewater using
86 conventional wastewater treatment methods. It is estimated that around 10% of dyes
87 used in textile dyeing procedures do not adhere to fibers and are thus discharged into
88 the environment (Liu et al., 2022). The recalcitrance of azo dyes, attributable to the
89 presence of azo bonds and sulphonate groups (Radhika and Aruna, 2022), and their
90 effects on the environment and human health makes their degradation not only a major
91 environmental concern but also a challenge (Katheresan et al., 2018).

92 Commercially accessible treatment approaches involve either removal or
93 destructive techniques depending on the content of the effluent. Coagulation (Hadadi
94 et al., 2022b; Sun et al., 2021; Tahraoui et al., 2022c), adsorption (Bouchelkia et al.,
95 2022; Imessaoudene et al., 2022), and membrane separations (Dasgupta et al., 2015)
96 are frequent removal procedures, whereas biological treatments (Adenan et al., 2022),
97 advanced oxidation processes (Muniyasamy et al., 2020), cavitation (Zampeta et al.,
98 2021), and incineration are destructive approaches. Regardless of the evolution of

technologies, there will always be a requirement for the use of coagulation in water and wastewater treatment, since it is regarded one of the simplest and cost-effective methods for enhancing the removal of pollutants from water (Kristianto et al., 2019).

Coagulation-flocculation technique refers to a physico-chemical process involving the use of a coagulant that neutralizes the negative charges in the polluted water, thereby reducing the electrostatic repulsion of the electric double layer; this is known as the destabilization process, it begins with an increment in ionic strength, which helps to promote double-layer compression, and/or with neutralization process of the particles surface charge by adsorption of anions (Alnawajha et al., 2022). These destabilized particles aggregate to form more or less large flocs via free precipitation or air flotation; these flocs are finally separated from the contaminated water (Han et al., 2022). Coagulation–flocculation has been used efficiently in several industries because to its simplicity of operation, relatively easy installation, and few energy requirements. Additionally, owing to the process's adaptability, coagulation–flocculation may be employed as a pre-treatment, a post-treatment, as well as the main treatment of wastewater (Vicente et al., 2022).

In reality, the most often employed chemical coagulants are divided into two groups: those consisting of aluminum, such as aluminum sulfate, sodium aluminate and aluminum chloride, and those derived from iron salts, such as ferric sulfate, ferric chloride, ferrous sulfate, or ferric chloride sulfate. Rarely is the usage of these compounds without consequences. Numerous environmental issues relating to the long-term toxicity of coagulants/flocculants are currently being explored, particularly for environmental observers worldwide. In addition to environmental impacts, there are also health concerns related to their use, metallic-based coagulants/flocculants are resistant to biodegradation and degradation, and when absorbed, their residuals in drinking water may have a direct impact on human health and accumulate in body cells. Indicators of the impact of chemical coagulants/flocculants on human health include malfunction of the central nervous system, dementia, Alzheimer's disease, and extreme shaking (Hadadi et al., 2022a). It is also known that they have several disadvantages, including high cost and high sludge production, which lead to additional water treatment (Zhang et al., 2022).

Biocoagulants and bioflocculants may be a viable substitute for chemical coagulants and flocculants to minimize environmental pollution and health hazards

related with their usage (Šuvalija et al., 2022). Biocoagulants and bioflocclulants are derived from living organisms or their components and are completely organic and biodegradable; hence, they are ecologically beneficial and have a negligible effect on human health (Adnan et al., 2017). Therefore, to develop these eco-friendly materials, several steps must be followed before they are used in treatment processing units. Many biocoagulants and bioflocclulants produced from various sources have previously been studied and have shown strong promise as alternatives to chemicals that are currently widely used, including *Moringa oleifera*, a highly promising alternative (Hadadi et al., 2022b; Kapse and Samadder, 2021; Nhut et al., 2021), rice starch (Teh et al., 2014), *Lens culinaris* (Chua et al., 2019), potato starch (Lapointe and Barbeau, 2017), *Dillenia indica* (Manholer et al., 2019), *Jatropha curcas* (Abidin et al., 2011), *Nephelium lappaceum* (Zurina et al., 2014), etc. Plant-based coagulants are easy to use, need little processing, and have the potential to provide a sustainable treatment solution. Despite the fact that a number of biocoagulants have been widely explored for practical applications, only a handful have been investigated in detail (Chethana et al., 2016).

In this research, we investigate the efficacy of a novel biocoagulant, *Pinus halepensis* Mill. seed extract, in treating synthetic water containing Congo red, a well-known carcinogenic and poisonous azo dye. As far as we know, the use of this biomaterial as a coagulant for the removal of dyes has not been previously reported, and biocoagulation investigations have shown very little interest in it (Hadadi et al., 2022a). *Pinus halepensis* Mill., commonly referred to as Aleppo pine, is the most abundant tree in the Mediterranean Basin, particularly in Algeria and Tunisia, and is a member of the 62 Pinaceae family (Ávila et al., 2022). These trees are characterized by their rapid growth, high propagule production, and adaptability to their native areas (Bello-Rodríguez et al., 2020). It has been reported that seeds exhibit a high proteins content (Al-Ismail et al., 2018), making them potential candidates as biocoagulant. The use of an active coagulant in the form of an extract has been favored over the direct use of seed powder; this will decrease the amount of organic matter associated with active coagulant substances, which increases BOD and COD levels in treated water (Baptista et al., 2017).

In this work, we investigated the influence of parameters such as coagulant dosage, initial pH, NaCl concentration, slow stirring speed and duration, solution

temperature and initial dye concentration on the Congo red removal efficiency. Moreover, a Support Vector Machine (SVM) coupled with the Gray Wolf Optimizer (GWO) was used to predict the removal rate of Congo red based on the optimized parameters of the biocoagulation process. Whereas SVM has lately garnered a significant deal of interest as an excellent modeling technique for water treatment systems, GWO technique has been utilized to handle a broad range of optimization problems, such as enhancing machine learning performance by optimizing model hyper-parameters. To our knowledge, such work has never been done before.

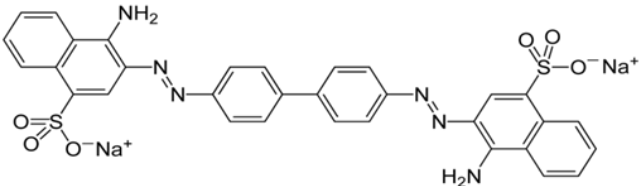
2. Material and methods

2.1. Chemicals and materials

Hydrochloric acid (HCl), sodium hydroxide (NaOH), Hexane, Bradford reagent, Albumin from bovine serum (BSA), Iron (III) chloride hexahydrate ($\text{FeCl}_3 \cdot 6 \text{H}_2\text{O}$), of high purity ($\geq 99\%$). and NaCl (all from Sigma Aldrich Chemical Company, USA) were employed for this investigation; Congo red was purchased from Biochem-Chemopharma, France.

Congo red dye was chosen as the model substance in this research and was dissolved in distilled water at a concentration of 1 g L^{-1} ; this stock solution was then diluted to generate solutions with the desired concentrations, and the required pH value was adjusted by using either 0.1 M HCl or NaOH solutions. Detailed informations about the structure and characteristics of the dye are presented in **Table 1**.

Table 1 Congo red properties

Dye	Congo red
Chemical class	Di-azo dye
Chemical formula	$\text{C}_{32}\text{H}_{22}\text{N}_6\text{Na}_2\text{O}_6\text{S}_2$
Molar mass (mol/g)	696.665
Maximum wavelength absorbance (λ_{max})	500 nm
Dye content	+ 75 %
Color change at pH	At [pH < 3.0] → Blue color/ At [pH > 5.0] → Red color
Chemical structure	

187

2.2. *Pinus halepensis* seed preparation and proximate composition analysis

188 *Pinus halepensis* Mill. seeds were purchased from a local herbal market,
189 thoroughly cleaned using distilled water to remove dust and impurities, oven-dried at
190 40°C for 24 hours (Memmert GmbH + Co.KG, Germany), crushed and powdered using
191 a domestic food processor, and sieved through a 500 µm sieve to promote the full
192 solubilization of active components in the coagulant (Hadadi et al., 2022a). To avoid
193 any deterioration of the active ingredients, the obtained powder was stored in sealed
194 amber-glass vial under refrigeration (4°C) until analysis. Moisture and ash contents
195 were determined using the AOAC method: about 3 g of the sample were dried at 105°C
196 during 3 hours before being transferred to a desiccator to cool. The moisture content
197 per 100 g of sample was estimated as the percentage change in weight before and
198 after oven drying. Ash content was determined by incinerating 5 g of the sample in a
199 muffle furnace (Nabertherm GmbH, Lilienthal, Germany) at 550°C for 6 h. The total
200 ash per 100 g of sample was represented as the weight of the greyish-white residue
201 obtained. Crude fat was determined using a Soxhlet apparatus; 20 g of the sample
202 was extracted in hexane under reflux for 8 h, and the extract was quantified as crude
203 fat per 100 g of the sample. Proteins content was expressed using the Bradford method
204 (Kielkopf et al., 2020), total carbohydrates were determined by difference.

205

2.3. Coagulant extraction

206 Salt extraction is recognized as a good approach for isolating proteins that may
207 behave as a polyelectrolyte during the coagulation process. According to previous
208 studies, NaCl was selected as the most suitable salt, owing to its availability and
209 economic advantages (Dalvand et al., 2016; Kristianto et al., 2019). The extraction was
210 performed following the steps shown in **Fig. 1**: 5 g of *Pinus halepensis* Mill. seed
211 powder were stirred with 100 mL of 0.1 to 2 M NaCl solution for 30 minutes; the
212 obtained suspension was centrifuged (Hettich Lab Technology, France) at 1006 ×g for
213 10 min and filtered through 45 µm fiberglass. To improve repeatability and avoid aging
214 effects such as pH, viscosity, and coagulation effectiveness changes caused by
215 microbial biodegradation during storage process, a fresh solution of the coagulant was
216 prepared for each sequence of experiments, the resulting extract is referred to as
217 PhsEXT.

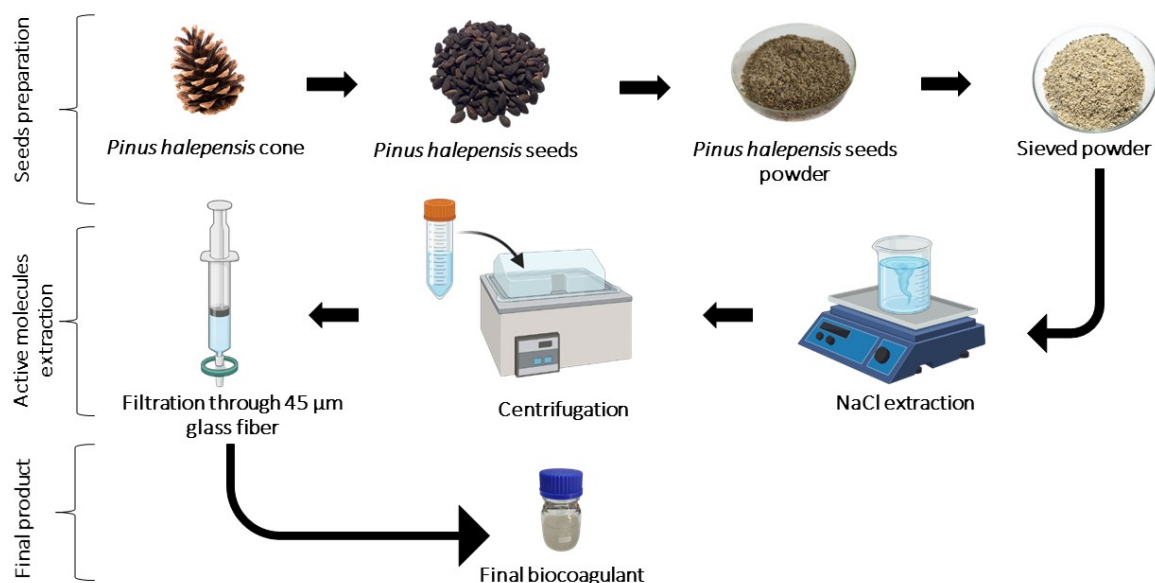


Fig. 1. Biocoagulant preparation steps.

2.4. Experimental procedure

Coagulation experiments were undertaken by using one-factor-at-a-time (OFAT) method, the trials were performed in 1 L beakers using a jar-test apparatus (VELP Scientifica Srl, Italy), each beaker was filled with 200 mL of the dye solution at desired concentrations (50 to 170 mg L⁻¹), pH values (3 to 10), dosages of freshly prepared PhsEXT (3 to 12 mL L⁻¹) and temperatures (10 to 60°C). The biocoagulant-dye mixture was rapidly agitated at 200 rpm for 3 min, then the mixing was reduced to lower speeds (0 to 110 rpm) for 0 to 30 min; flocs were given time to settle (for 0 to 40 min). Following that, samples (20 mL) were collected using a volumetric pipette at 3 cm below the mixture surface (Dalvand et al., 2016) and then centrifuged (1006 xg for 10 min). The final concentrations of the dye were determined using a spectrophotometer (Agilent Cary 60 UV-Vis, USA). The measurement is performed at 500 nm for the pH range 5–10 and at 562 nm for pH range 3–4. At these wavelengths, pH-specific calibration curves are developed and used. All studies were repeated three times. The % removal of Congo red dye R (%) was calculated using Eq. (1):

$$R(\%) = \frac{C - C_f}{C} \times 100 \quad (1)$$

where C (mg L^{-1}) and C_f (mg L^{-1}) represent the initial and residual dye concentrations, respectively.

2.5. Morphology of flocs

For morphological observations, an optical microscope (Kern & Sohn, Germany) equipped with a mobile camera was used. A drop containing flocs of a fresh dye-PhsEXT mixture was carefully placed on a glass slide and covered with a coverslip. It was immediately observed at x100 magnification to get the pictures.

2.6. Support vector machine (SVM)

Vapnik developed the support vector machine in the 1990s (Vapnik et al., 1996), it is founded on the statistical learning theory (SLT) techniques and structural risk minimisation (SRM) concept (Wang et al., 2022). Its primary applications were regression analysis and non-linear classification (Bargagli Stoffi et al., 2022). A training data set of N points (X_i, Y_i) is examined in this technique, with $i = 1, N$. X denotes the inputs of the model and Y its output. A SVM model appears like:

$$y(x) = \omega^T \phi(x) + b \quad (2)$$

where $\phi(\cdot): R^n \rightarrow R^m$ is a non-linear function that maps the finite dimensional space entry into a higher dimensional space that is implicitly created, ω represents a weight vector, and b is the bias (Suykens et al., 2002; Vapnik et al., 1996).

In this study, the SVM model was chosen for the prediction of the removal rate of Congo red by the PhsEXT using the Matlab R2020a software. For this purpose, the results of the parameter optimization (part "2.4. Experimental procedure") for the removal of Congo red were compiled into a single database, which has 8 input parameters and one parameter Release

The independent parameters were the slow stirring time (X1), the sedimentation time (X2), the initial concentration of Congo red (X3), the dose of biocoagulant (X4), the pH of the solution (X5), the concentration of NaCl (X6), The slow stirring speed (X7) and temperature (X8). In contrast, the dependent parameter was the removal rate of Congo red (Y).

To obtain the optimal result from SVM, the Gray Wolf Optimizer (GWO) algorithm was coupled with SVM (SVM_GWO) in order to optimize the parameters of each kernel

function. As a result of its remarkable capacity to enhance model performance via hyper-parameter optimization (Colombo, 2017; Mirjalili et al., 2014).

To construct the model, the MATLAB software Help guide was used, this design is shown in the following illustration:

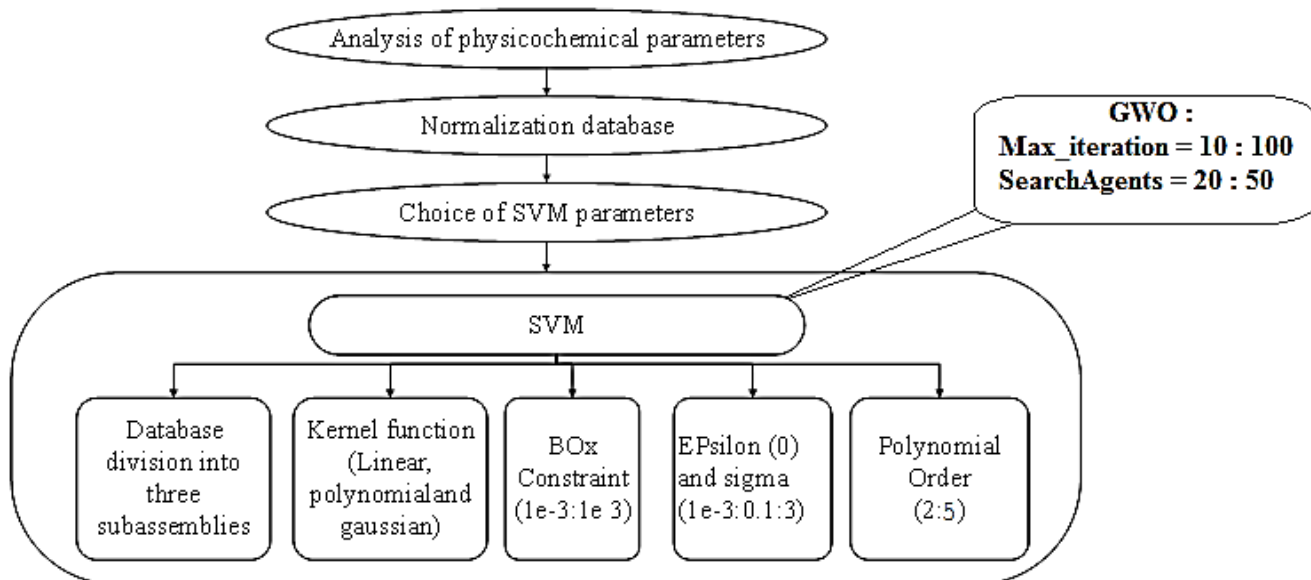


Fig. 2. Organization chart for SVM mode development and optimization.

Where:

- The database was normalized once in the interval $[-1, +1]$ using MATLAB's "mapminmax" function. Next, the database was split into two: 80% of the dataset for training and 20% of the validation samples.
- The kernel functions that have been selected in this study are as follows: (Benimam et al., 2020).

- Poly (polynomial)

$$k(X_i, X_j) = (ax^T + c)^d \quad (3)$$

- Linear

$$k(X_i, X_j) = x^T y + c \quad (4)$$

- Gaussian

$$k(X_i, X_j) = \frac{1}{\sigma\sqrt{2\pi}} \exp\left\{\frac{-X_i - X_j^2}{2\sigma^2}\right\} \quad (5)$$

with $C = \text{BOxConstraint}$, $d = \text{Polynomial Order}$, $\varepsilon = \text{epsilon}$ and $\sigma^2 = \text{sigma}$ where d , c , ε , and σ^2 are the defined kernel parameters.

2.7. Statistical criteria

Statistical criteria were used to evaluate the performance and select the best model, including the Correlation Coefficient (R), the Coefficient of Determination (R^2), the Adjusted Coefficient (R^2_{adj}), the Mean Square Error (MSE), the Root Mean Square Error (RMSE), and the Mean Absolute Error (MAE). Error Standard of Prediction (ESP) and Error Prediction of Model (EPM) were also considered. These criteria are calculated considering the following equations (Bousselma et al., 2021 ; Tahraoui et al., 2020, 2021a, 2021b, 2022a, 2022b).

$$R^2_{adj} = 1 - \frac{(1-R^2)(N-1)}{N-K-1} \quad (6)$$

$$RMSE = \sqrt{\left(\frac{1}{N}\right) \left(\sum_{i=1}^N \left[(y_{\text{exp}} - y_{\text{pred}}) \right]^2 \right)} \quad (7)$$

$$MSE = \left(\frac{1}{N} \right) \left(\sum_{i=1}^N (y_{\text{exp}} - y_{\text{pred}})^2 \right) \quad (8)$$

$$MAE = \left(\frac{1}{N} \right) \sum_{i=1}^N |y_{\text{exp}} - y_{\text{pred}}| \quad (9)$$

$$ESP(\%) = \frac{RMSE}{\bar{y}_{\text{exp}}} \times 100 \quad (10)$$

$$EPM(\%) = \frac{100}{N} \sum_{i=1}^N \left| \frac{(y_{\text{exp}} - y_{\text{pred}})}{y_{\text{exp}}} \right| \quad (11)$$

Where N is the number of data samples; K is the number of variables (inputs); \bar{y}_{exp} and \bar{y}_{pred} are the experimental and the predicted values respectively; \bar{y}_{exp} and \bar{y}_{pred} are the average values of the experimental and the predicted values, respectively (Bousselma et al., 2021; Tahraoui et al., 2021a, 2021b, 2022a, 2022b).

3. Results and discussion

3.1. Physicochemical characterization

The physicochemical characteristics of *Pinus halepensis* Mill. seeds are presented in **Table 2**.

The moisture level was 2.3 g/100g, while the ash content was 4.6 g/100g. The seeds had a considerable amount of fat: 31.10 g/100 g. Although pine seeds are typically rich in oils, their composition varies based on species and environmental factors (Dziedziński et al., 2021). Total carbohydrates were 31.4 g/100 g (per difference). The proximate proteins content reached 30.6 g/100 g. Tukan et al. (2013) observed that the proteins level of raw or cooked *Pinus halepensis* Mill. seeds could reach more than 29%; these data suggest a high concentration of proteins capable of acting as a coagulant agent in our investigation.

Table 2 Chemical composition of Aleppo Pine (*Pinus halepensis* Mill.) seeds. (mean±SD, n= 3)

Composition	Percentage
Dry matter	97.7±0.6
Ash content	4.6±0.1
Crude proteins	30.6±1.2
Fat	31.1±1.2
Total carbohydrates (by difference)	31.4±1.2

Fig. 3 shows that numerous main peaks with several intensities were detected at different frequencies in the FTIR spectrum. The broad peak at 3281 cm⁻¹ can be ascribed to the stretching vibrations of the –OH groups indicating the presence of the functional groups alcohol, phenol, carboxylic group and –NH stretching of amide and amines groups (Ghodke et al., 2021), which appear predominantly in the carbohydrates, polysaccharides (Saldarriaga-Hernández et al., 2021), proteins and fatty acid structures present in the *Pinus halepensis* Mill. seeds. The sharp peak in the vicinity of 2922 cm⁻¹ was related to the C-H stretching of either alkane (Ghodke et al., 2021) or carboxylic acid (El-Din et al., 2017). 2852 cm⁻¹ was related to the –CH– and CH₂ stretching vibrations found in fatty acids. In the region between 1743 cm⁻¹ and

1633 cm^{-1} , there are strong peaks linked to C=O bond stretching, carbonyl group is present in proteins and fatty acids. The peak at 1537 cm^{-1} is attributed to the bending of NH_2 (amine) group (Putra et al., 2020); the presence of this band demonstrates that *Pinus halepensis* Mill. seeds have a protein structure containing amino groups. Bands at 1455 cm^{-1} and 1235 cm^{-1} correspond to the C-O stretching of carboxylic acids and phenolic compounds, while that at 1058 cm^{-1} correspond to the C-O stretching of polysaccharides (Araújo et al., 2016). Similar FTIR spectra have been observed in previous studies on natural coagulants (Amran et al., 2021; Hussain and Haydar, 2019).

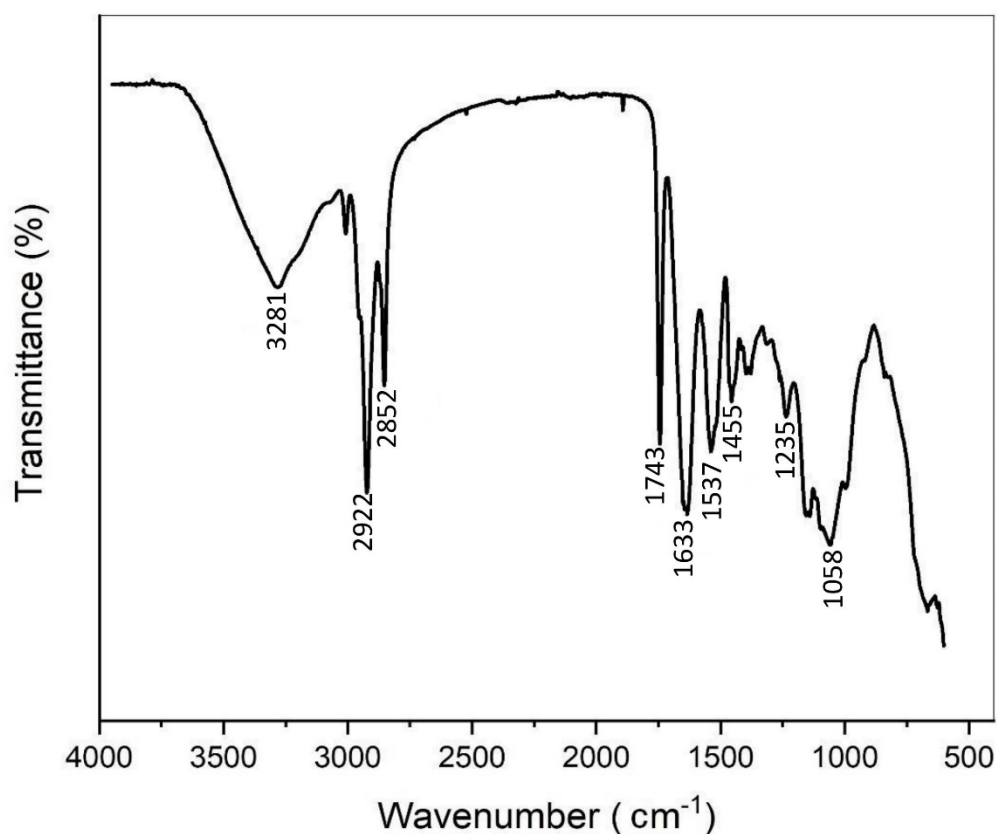


Fig. 3. FTIR spectra of *Pinus halepensis* Mill. seeds.

3.2. Factors affecting the coagulation process

3.2.1. Effect of initial pH on Congo red removal

pH is a crucial parameter in the coagulation–flocculation process since it influences the biocoagulant surface charge and the stabilization of the dye wastewater. **Fig. 4(a)** depicts the influence of pH throughout a pH range of 3 to 10 (Due to Congo red precipitation, lower pH values were neglected); very acidic conditions promote effective Congo red removal, with a maximum percentage of 80.46% at pH = 3. The removal rate decreases dramatically as pH continues to rise. This result is consistent with previous studies (Chethana et al., 2016; Tie et al., 2015b); Since proteins are believed to be the active agent in coagulation, their amino groups may get protonated under acidic conditions, enhancing their interaction with the anionic portion of the dye (sulfite SO_3^{2-} groups). A further rise in pH is expected to cause proteins carboxyl groups to become negatively charged (COO^-), hence increasing the solubility of Congo red due to electrostatic repulsion. The proteinaceous profile of *Pinus halepensis* seeds supported by FTIR and proximate composition analysis results corroborate these assumptions. (Abidin et al., 2011; Bahrodin et al., 2021) reported that the coagulation mechanism is charge neutralization when the difference between maximum removal and minimum removal by using different pH is around 50% or more, which is the case in our investigation. Also, bridging cannot be considered as a possible mechanism because unlike charge neutralization, bridging is least affected by pH. however, at lower pH, the polymeric chains responsible for interparticle bridging will expand and be able to attach to additional pollutants (Momeni et al., 2018; Zaidi et al., 2022). Using aluminum sulfate, Vijayaraghavan et al. (2015) observed a 74% Congo red removal rate under the same acidic conditions and initial dye concentration of 50 mg L^{-1} , while Kristianto et al. (2021) reported that ferric chloride removed 30% of the dye (Congo red initial concentration = 50 mg L^{-1} , pH = 6.5).

3.2.2. Effect of coagulant dosage on Congo red removal

Coagulant dosage is a primordial parameter since it determines the cost of the coagulation–flocculation process (Tie et al., 2015a). The experiment was carried out to identify the optimal dose of PhsEXT in terms of Congo red elimination. 50 mg L^{-1} of Congo red were treated with an increasing dose of coagulant (3 to 12 mL L^{-1}). We opted to represent the coagulant dosage in units of mL L^{-1} rather than mg L^{-1} since the

filtering step retains around 70% of the insoluble *Pinus halepensis* Mill. seed powder during PhsEXT preparation (Nhut et al., 2021).

From **Fig. 4(b)**, it is observed that the increase in the biocoagulant dose increases the percentage removal of Congo red until reaching a plateau, after which additional increases in dosage did not improve the percentage removal; However, Congo red removal decreased when the dosage was further increased up to 12 mL/L (results not shown), this is explained by the fact that the main concept of coagulation is the destabilization of colloidal matter and suspended particles by the introduction of positive species. However, when the coagulant dosage increases, there will be an excess of positive ions, leading the particles to repel one another and the solution to re-stabilize. A dose of 10 mL L⁻¹ gives an optimal dye removal rate of 81.17 %. The interaction between the positive charges of the amino groups and the negative charges of the anionic dye, as previously stated, is thought to explain the coagulation process observed in this work, more dye molecules are destabilized by electrostatic attraction when the coagulant dose is increased, resulting in greater charge neutralization and, thus, a higher dye elimination % (Chethana et al., 2016; Dalvand et al., 2016; Hadadi et al., 2022a; Pardede et al., 2018). Shamsnejati et al. (2015) reported the use of *Ocimum basilicum* as a biocoagulant to eliminate Congo red, achieving a maximum color removal of 68.5% using 1.6 mg L⁻¹ (initial Congo red concentration = 50 mg L⁻¹). Under acidic conditions (pH = 3), a solution of 2 % potato starch was found to remove about 50% of Congo red (Pardede et al., 2018). Mishra et al. (2004) observed that adding 10 mg L⁻¹ of *Plantago psyllium* mucilage to an initial dye concentration of 1 mg L⁻¹ led to the maximum elimination of golden yellow and reactive black, with 71 % and 35 %, respectively. *Moringa oleifera* and *Phaseolus vulgaris* extracts at 30 mg L⁻¹ removed 83 % and 73 % of Congo red, respectively, with an initial dye concentration of 50 mg L⁻¹ and pH = 4. (Vijayaraghavan and Shanthakumar, 2015). In comparison to previous studies, PhsEXT exhibits a high efficiency in the removal of Congo red dye.

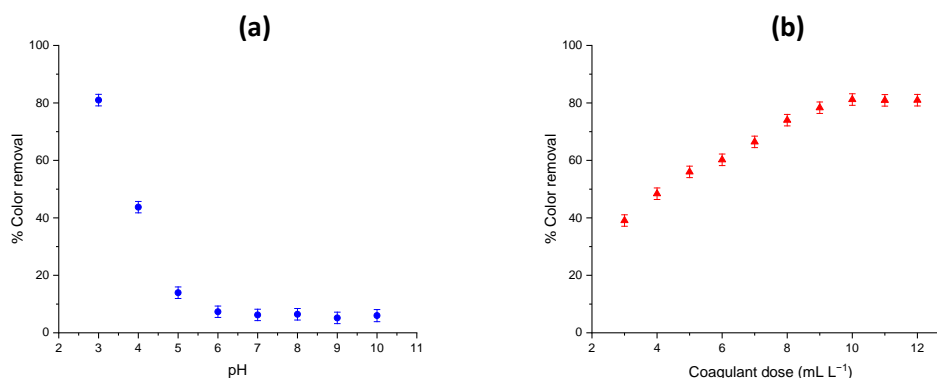


Fig. 4. Parameters affecting the removal of Congo red dye by the biocoagulant, (a) Effect of initial pH of Congo red solutions, (b) Effect of biocoagulant dosage.

3.2.3. Effect of initial Congo red concentration

To examine the effect of the initial dye concentration on the coagulation efficiency, optimal conditions found earlier (pH = 3, coagulant dose = 10 mL L⁻¹) were applied to different concentrations of Congo red (50 to 170 mg L⁻¹). **Fig. 5(a)** clearly shows that increasing the initial Congo red concentration resulted in a decrease in the percentage of dye elimination from 80.78 % to 43.61 %.; this trend was noticed in earlier studies (Beltrán et al., 2009; Chethana et al., 2016). As the dye concentration increases, the coagulant dose becomes insufficient for neutralizing the negative charges in Congo red dye, and PhEXT becomes exhausted (Beltrán et al., 2009). In conclusion, treating dye wastewater with a higher initial concentration may need a larger dosage of natural coagulant by providing more adsorption sites.

3.2.4. Effect of NaCl concentration

Several NaCl solutions with concentrations of 0.1; 0.5; 1; 1.5; and 2 M were selected to examine the effect of salt solution concentration on coagulation efficiency. The results (**Fig. 5(b)**) shows that the coagulation effectiveness of the biocoagulant increases with an increase in salt concentration. Maximum dye removal (81.51%) was achieved at 1 M of NaCl. This phenomenon is thought to be caused by the salting-in mechanism, which refers to the process of increasing the ionic strength of a solution, hence boosting the solubility of the proteins present in *Pinus halepensis* Mill. seeds, which are believed to act as a coagulant agent (Dalvand et al., 2016; Madrona et al., 2010). A further increase in NaCl concentration is expected to result in the opposite phenomenon, salting out; at high salt concentrations, the solubility of proteins reduces

dramatically, resulting in poorer extraction and a low Congo red dye removal % (Megersa et al., 2019; Hadadi et al., 2022b). According to Dalvand et al. (2016) , when the concentration of NaCl rises, chloride ions may compete with dye molecules for attraction with the positive charges on the coagulant surface, resulting in decreased dye removal.

3.2.5. Effect of slow stirring speed on dye removal efficiency

Rapid mixing is often used to promote better chemical dispersion in the suspension, slow stirring is then applied to allow particles to aggregate in larger settleable flocs, According to **Fig. 5(c)**, At a slow agitation speed of 30 rpm, the highest dye removal percentage of 81.80 % was achieved; Increased stirring speed resulted in a decrease in dye removal; this might be attributable to the breakage of existing flocs because of disruptive forces (Teh et al., 2014).

3.2.6. Effect of slow stirring time and floc settling time on dye removal

The settling of generated flocs is the last phase in the coagulation-flocculation process. A faster floc settling rate is advantageous during the coagulation process and shows the efficiency of the coagulant (Daverey et al., 2019). The effect of flocculation mixing time and settling time on Congo red elimination percentages were studied ; time intervals ranging from 0 to 30 minutes were used (data not shown). flocs rapidly settled within the first 5 min, with little fluctuation after 10 min. This phenomenon might be explained by the rapid formation of aggregates of appropriate size that settle rapidly and easily.

3.2.7. Effect of solution temperature on the dye removal efficiency

Although temperature has not been extensively investigated in earlier studies, especially when the coagulation-flocculation process is carried out at temperatures higher than 25°C (Domínguez et al., 2005), given that some textile dyeing effluents are produced at relatively high temperatures, this parameter must be considered. Maintaining earlier parameters at their optimum (pH= 3, coagulant dosage= 10 mL/L, Initial Congo red concentration = 50 mg/L, NaCl concentration = 1 M, Slow stirring speed = 30 rpm, slow stirring time = 20 min, floc settling time = 30 min), temperature was varied from 10 to 60°C, **Fig. 5(d)** depicts the results. It is noteworthy that the dye removal percentage improves from 38.89% to 81.93% when the temperature is

increased from 10°C to 60°C; this may be explained by the effect of temperature on solution viscosity, which rises as temperature decreases, high viscosity has a negative influence on flocs' collision rates, while low temperature is thought to weaken particle aggregation in solution, resulting in poor Congo red removal. (Pritchard et al., 2010; Rodrigues et al., 2013; Tie et al., 2015a).

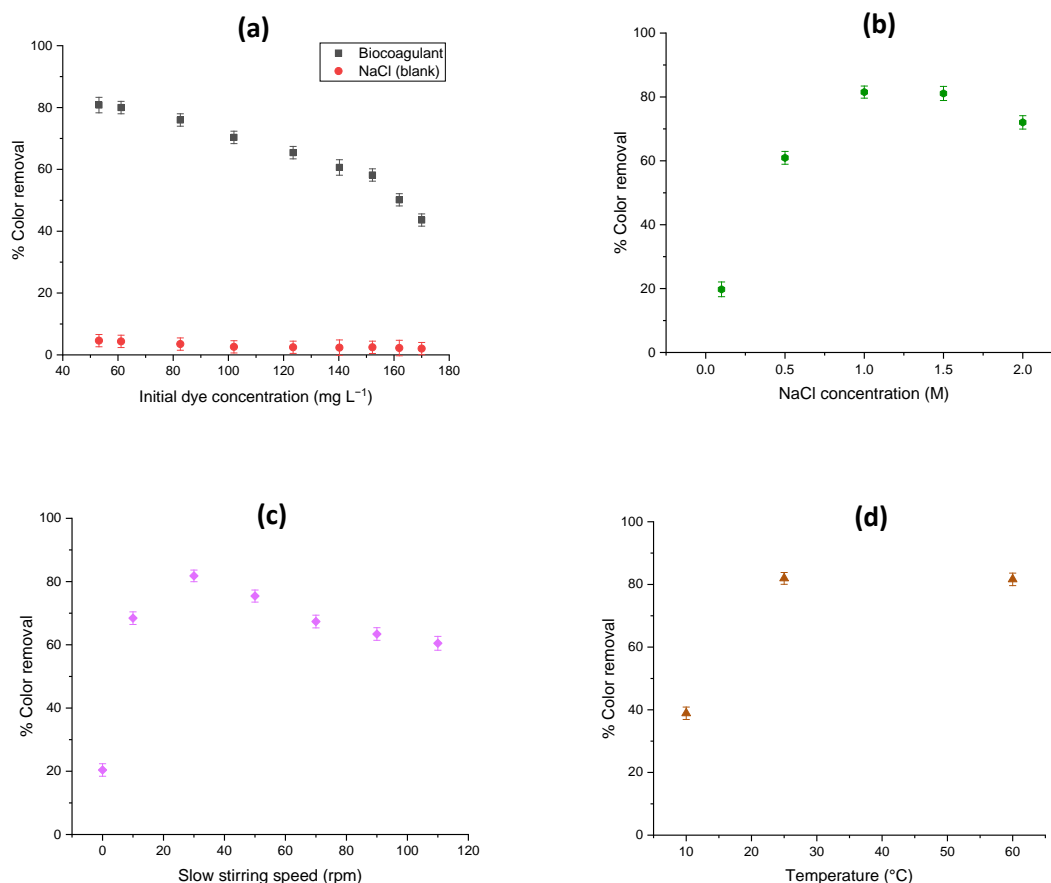


Fig. 5 (a) Effect of Congo red and NaCl (blank) concentrations, (b) Effect of extraction solution's concentration (NaCl), (c) Effect of slow stirring speed (flocculation step), (d) effect of Congo red solutions temperature. (Optimal conditions of each parameter were kept for the next step).

3.3. Morphology of flocs

The size and structure of flocs are considered to be critical to the efficient functioning of industrial units. The goal of water and wastewater treatment is to remove contaminants in the form of solid particles from polluted water. After the solid particles are formed, they may be separated from the treated water using sedimentation, flotation, filtration, and thickening methods. Consequently, the physical properties of

flocs are important in determining their removal efficacy. Using a light microscope, the formation of flocs was observed in this study for both FeCl_3 -dye and PhsEXT-dye (**Fig. 6**) (Szygula et al., 2009). Notably, the biocoagulant generated flocs that were thicker and denser than FeCl_3 , which produced flocs that were light, dispersed, and more fragile. These results suggest that flocs generated with a biocoagulant settle faster (Pan et al., 1999); This parameter indirectly measures the efficacy of the coagulation–flocculation process (Aziz and Ramli, 2017) and is a good indication of the suitability of *Pinus halepensis* Mill. seed-based biocoagulant as an alternative to chemical coagulants such as FeCl_3 .

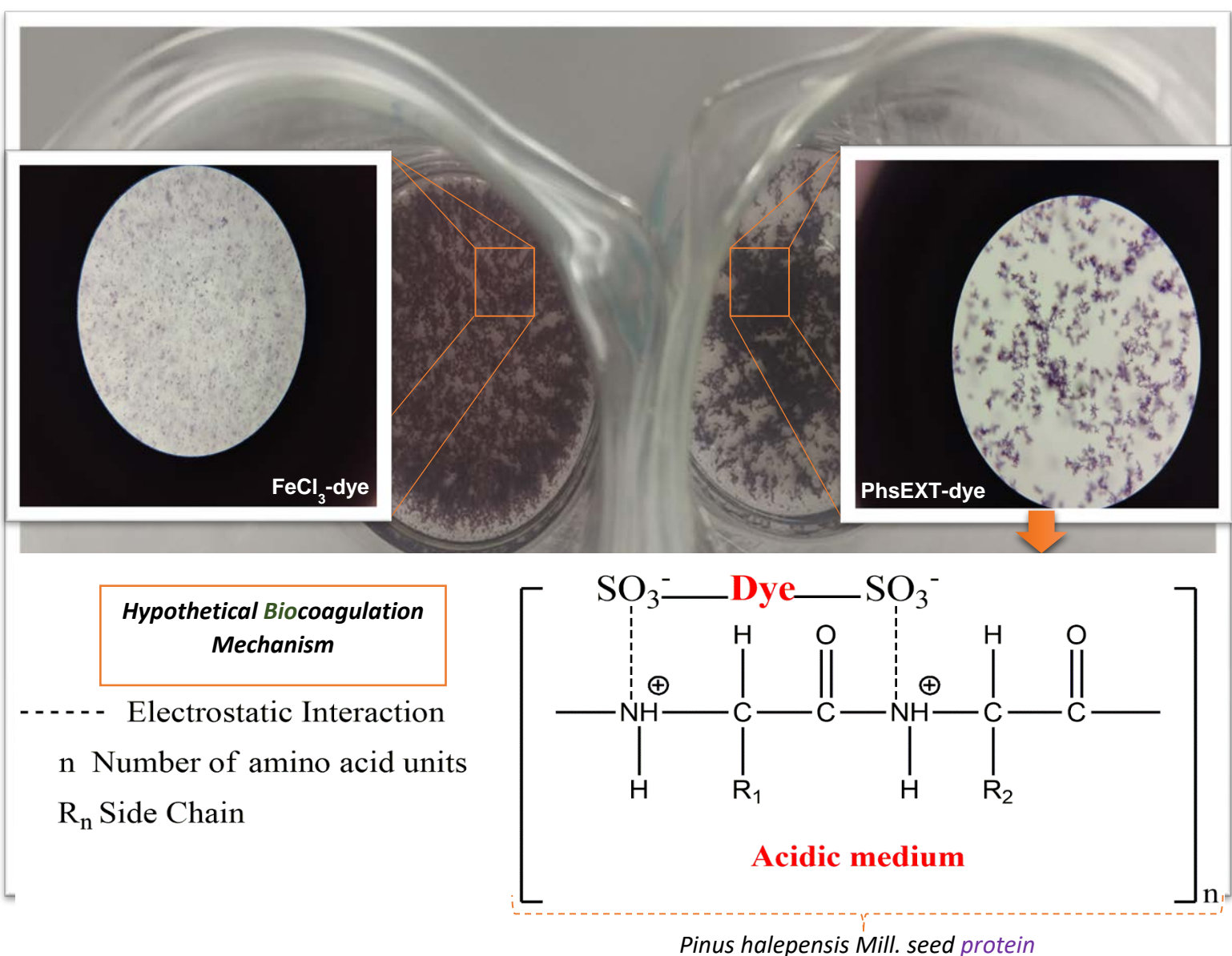


Fig. 6. Microscope observation of floc formation at 100× magnification (pH= 3, dosage 10 mL L⁻¹, C = 50 mg L⁻¹, sampling at 60 min) with hypothetical biocoagulation mechanism occurring in this study.

3.4. Congo red removal Rate modelling using a Support Vector Machine coupled with Gray Wolf Optimizer

In this part, 3 kernel functions were optimized, and each kernel synthesized by the variables must also be optimized: The linear function generated by BOxConstraint, epsilon, and sigma; the Gaussian function synthesized by BOxConstraint, epsilon, and sigma; and the polynomial function generated by BOxConstraint, epsilon, and PolynomialOrder, knowing that PolynomialOrder was optimized from 2 to 5. Using the GWO technique, the variables of each kernel function were optimized.

After acquiring the outcome of the learning phase, the result was confirmed using the validation database. In order to calculate R, R², R²adj, RMSE, MSE, EPM, ESP, and MAE, the generated results (predicted values) were compared with the experimental values in the two phases (the learning phase and the validation phase). The outcomes of these tests are shown in **Table 3**. Note that the findings were denormalized to their actual values in order to be compared to other models.

Table 3 Performances of the different tested SVM Kernel function.

GWO Max_iteration=100 SearchAgents_no=30											
Kernel function	C	ϵ	σ^2	d		R/R ² /R ² _{adj}			RMSE/MSE/EPM/ESP/MAE		
						Train	Val	All	Train	Val	All
Linear	540	208.1278	1.2000	/	45	0.7836	0.5543	0.7573	17.6421	14.4266	17.0584
						0.6140	0.3073	0.5735	311.2425	208.1278	290.9878
						0.5283	0.3073	0.5009	67.9624	15.6305	57.6829
									30.4879	20.8748	28.3954
									11.8560	11.1706	11.7213
Gaussian	1180	1.6758	1.2000	/	45	1.0000	0.9993	0.9998	0.1045	1.2945	0.5813
						1.0000	0.9986	0.9995	0.0109	1.6758	0.3379
						1.0000	0.9932	0.9995	0.0315	4.8643	0.9808
									0.1738	2.1594	0.9677
									0.0252	1.1094	0.2382
Polynomial	10	23.1264	/	4.8000	45	0.9945	0.8969	0.9917	2.8729	4.8090	3.3429
						0.9890	0.8044	0.9835	8.2534	23.1264	11.1748
						0.9865	0.0218	0.9807	7.4935	3.9188	6.7913
									5.1037	6.3647	5.5646
									1.7791	3.0117	2.0212

542

543 By comparing the coefficients and the statistical errors, it is obvious that the

544 Gaussian function gave the best result; this result is schematized graphically by **Fig.**

545 **7:**

546

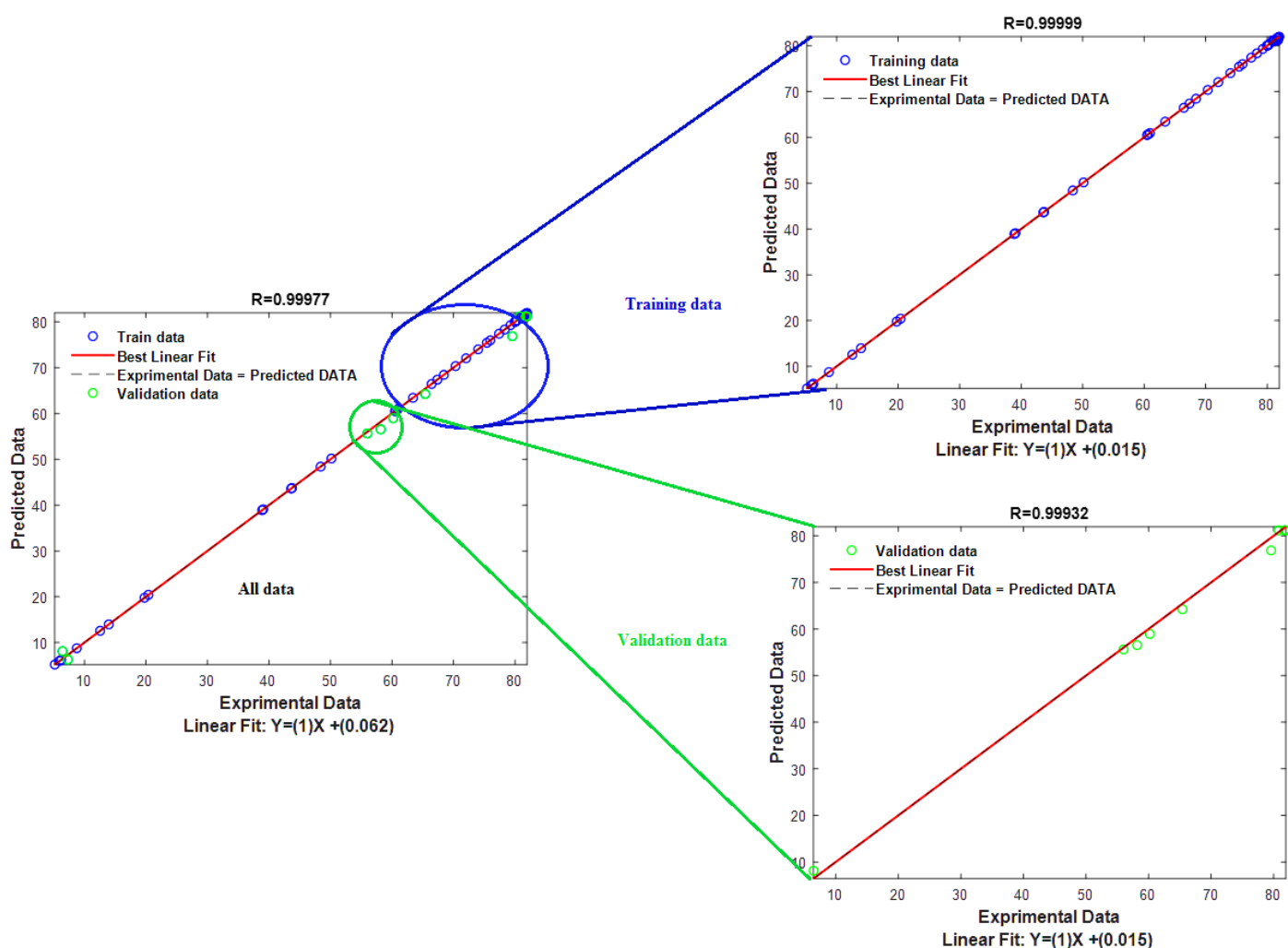


Fig. 7. The relationship between the measured dosage of coagulant and the SVM-estimated dose.

3.4.1. Model performance test

Interpolation was used to assess the performance of the generated SVM_GWO model. This was performed by using a cached database comprising 20 experimental data points that were not used during model training. **Table 4** summarizes the results in terms of coefficients and statistical errors.

559

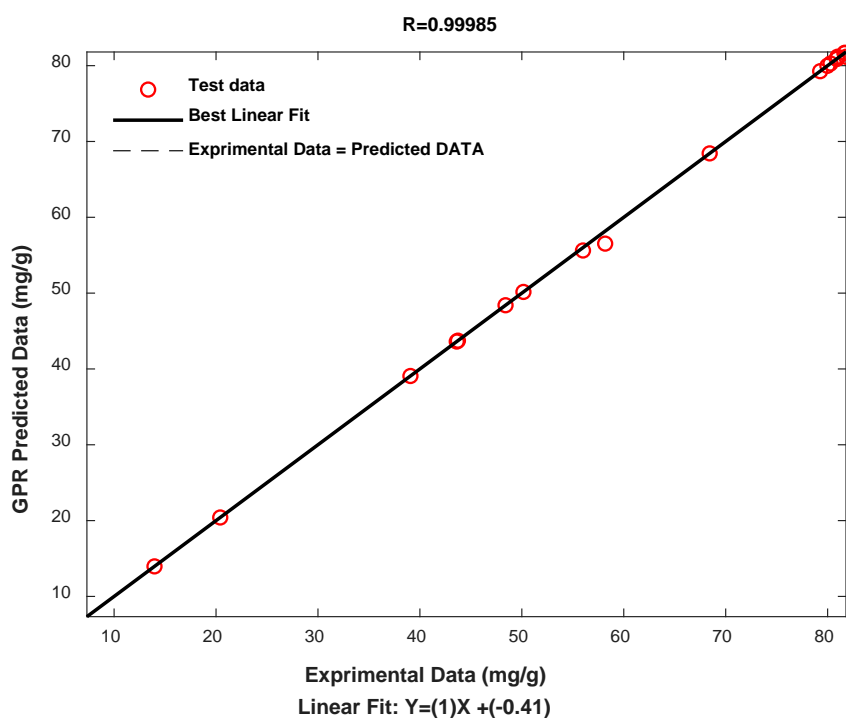
Table 4 Model test performance.

R/R ² / R ² _{adj}	RMSE/MSE/ EPM/ESP/MAE
ALL	ALL
0.9998	0.4675
0.9996	0.2186
0.9994	0.9364
	0.7945
	0.1951

560

561 The coefficients shown in **Table 4** demonstrate the effectiveness and
 562 performance of our model.

563 This result was represented graphically (**Fig. 8**) in terms of the experimental
 564 values and the predicted values.



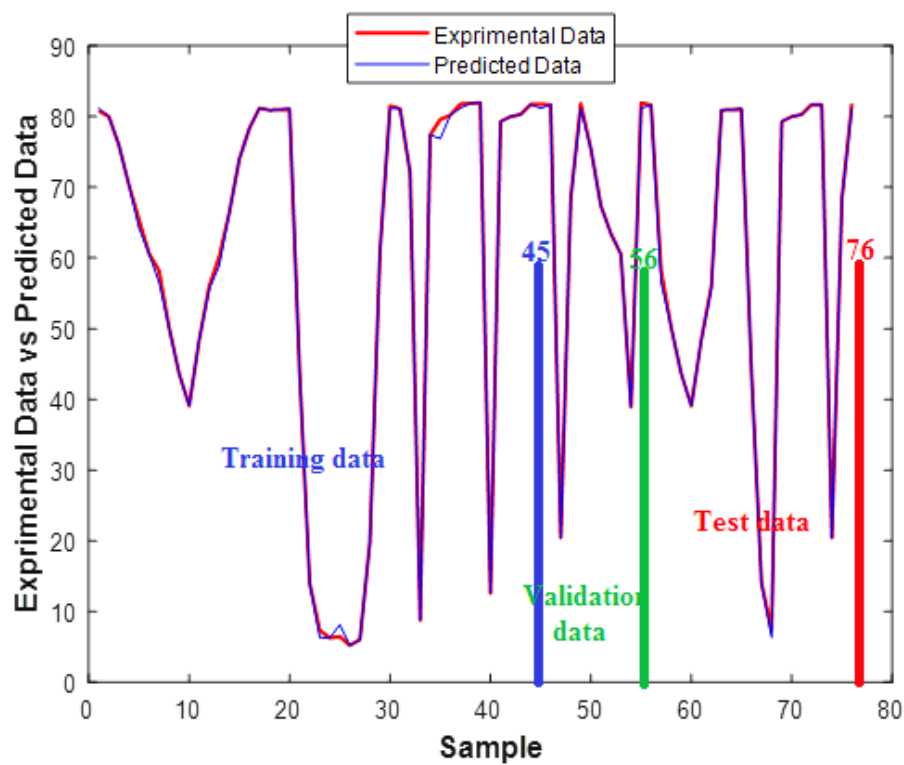
565

566 **Fig. 8.** Comparison between experimental and predicted values to assess
 567 performance.

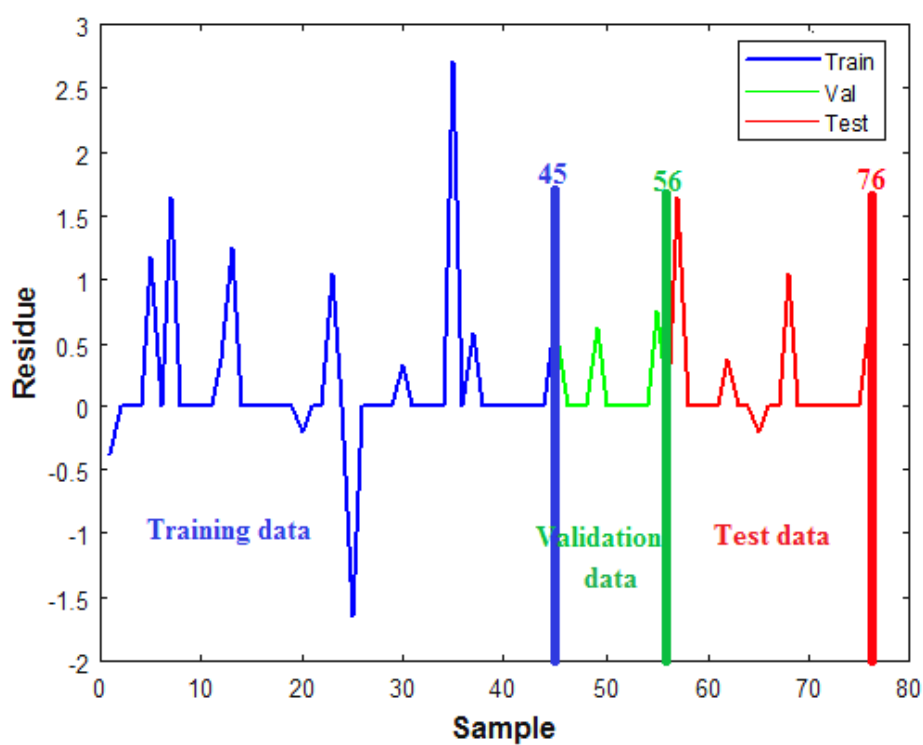
3.4.2. *Residues study*

The residuals approach was used in this study to investigate the relationship between the experimental and predicted values on the one hand, and the efficiency and performance of the chosen model on the other (Tahraoui et al., 2021b, 2022b). For this purpose, the experimental and predicted values were plotted in parallel as a function of samples (**Fig. 9(a)**) for all data (including data training, data validation and data test performance) (Bousselma et al., 2021; Tahraoui et al., 2022a).

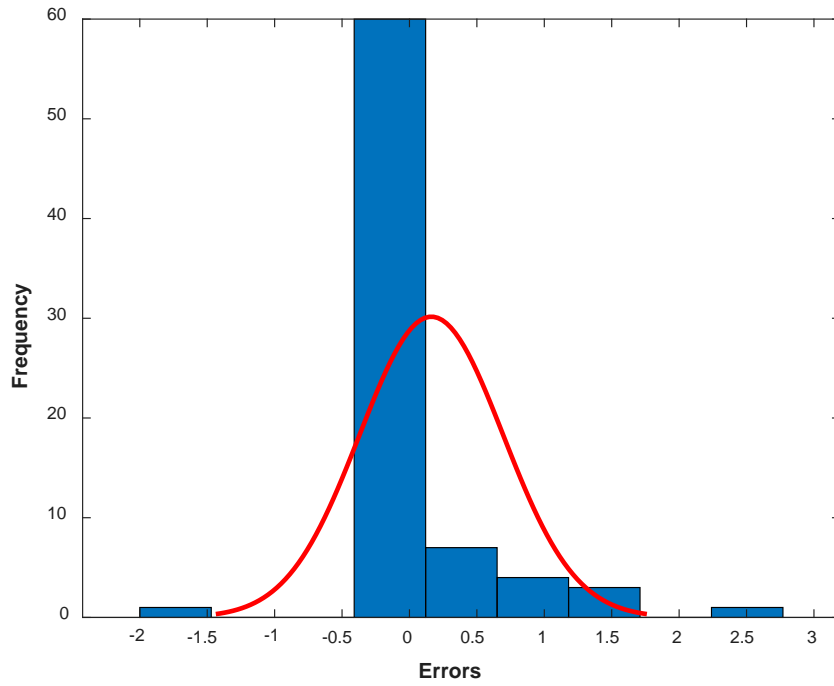
In contrast, for all data, the error was determined as the difference between the experimental and predicted values (including data training, data validation and data test performance). This error was plotted graphically (**Fig. 9(b), (c) and (d)**) by three methods (residue, frequency and instances) (Tahraoui et al., 2021a, 2021b, 2022b).



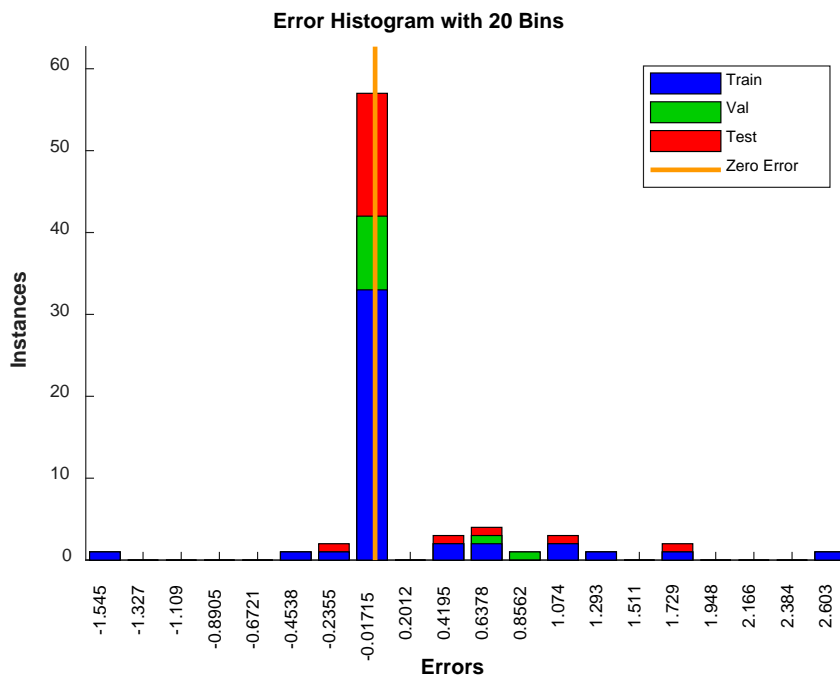
(a)



(b)



(c)



(d)

Fig. 9. Residuals relating to the models established by the different techniques according to the estimated values: (a) Relationship between experimental and anticipated sample data, (b) Residues relating to the models established, (c) Frequency distribution of errors, and (d) Instances distribution of errors.

Fig. 9(a) shows the strong convergence between the experimental values and the predicted values, confirming once again the efficiency of the obtained model.

Moreover, **Fig. 9(b)** shows the small errors obtained in the three phases. Indeed, in the learning phase the error did not exceed 3%, the error values were 1% in the validation phase, and 2% for the test phase. It can therefore be concluded that the errors obtained from our model are very small. This was confirmed by examining **Fig. 9(c) and (d)**, where **Fig. 9(c)** shows that the high frequency was obtained at error 0. Similarly for **Fig. 9(d)**, where most errors were around zero for all three phases (training, validation, and testing data). All these demonstrations and interpretations strongly demonstrate the efficiency and performance of our model.

3.5. Optimization of the optimal analysis and Validation

An optimization method was carried out using GWO to find the optimal conditions for the elimination of Congo red by the biocoagulant.

The optimization results revealed ideal conditions for small concentrations, namely up to 150 mg/L ($X_1 = 20$ min, $X_2 = 30$ min, $X_3 = 50$ and 150 mg L^{-1} , $X_4 = 10 \text{ mL L}^{-1}$, $X_5 = 3$, $X_6 = 1$, $X_7 = 30$ rpm, and $X_8 = 25^\circ\text{C}$). For concentrations greater than 150 mg L^{-1} , the same preliminary conditions as those obtained for the concentration less than 150 mg L^{-1} apply, the only difference is that the temperature must be increased to 60°C ($X_8 = 60^\circ\text{C}$) for an elimination rate of 53.23 % to be achieved. These findings were validated in the laboratory by applying the ideal conditions at various doses (50, 150, and 170 mg L^{-1}). The optimization results are shown in **Table 5** with an error rate of less than 2%, demonstrating our model's effectiveness once again.

604 **Table 5** Results of the removal rate of Congo red under the optimal conditions.

GWO: X1 = 20 min, X2 = 30 min, X3 = 50 mg L ⁻¹ , X4 = 10 ml L ⁻¹ , X5 = 3, X6 = 1 M, X7 = 30 rpm and X8 = 25°C	
The predicted removal rate of Congo red (%)	81.17
The experimental removal rate of Congo red	81.93
Error (%)	0.79
GWO: X1 = 20 min, X2 = 30 min, X3 = 150 mg L ⁻¹ , X4 = 10 mL L ⁻¹ , X5 = 3, X6 = 1 M, X7= 30 rpm and X8= 25°C	
The predicted removal rate of Congo red (%)	56.52
The experimental removal rate of Congo red	58.17
Error (%)	1.65
GWO: X1 = 20 min, X2 = 30 min, X3 = 170 mg L ⁻¹ , X4 = 10 mL L ⁻¹ , X5 = 3, X6 = 1 M, X7= 30 rpm and X8 = 60°C	
The predicted removal rate of Congo red (%)	53.23
The experimental removal rate of Congo red (%)	51.83
Error (%)	1.4

605

606 3.6. *Comparison of Pinus halepensis Mill. seed extract coagulating performances*
607 *with ferric chloride (FeCl₃)*

608 For comparative purposes, 50 mg L⁻¹ of Congo red dye were treated with different
609 amounts of ferric chloride (results not shown), to do so, optimal conditions obtained
610 earlier were taken into consideration. Using the Imhoff cones method, the quantity of
611 wet sludge generated by the two coagulants (FeCl₃ and PhsEXT) was also studied.
612 According to **Table 6**, PhsEXT and FeCl₃ demonstrated nearly identical removal rates
613 (81.22 % and 83.78 %, respectively); FeCl₃ generated higher sludge quantity (about
614 18 mL more) comparing to PhsEXT. Similar results have been reported by (Choudhary
615 et al., 2019; Kristianto et al., 2019). Organic polymers typically generate less sludge
616 than chemical coagulants since they don't contribute in adding weight to the water or
617 react chemically with some other ions to form precipitates. Thus, the sludge formed by
618 PhsEXT was volume-reduced and compressed. This can also be attributed to the

difference between flocs formed when FeCl_3 and the biocoagulant were used (Dalvand et al., 2016). This shows that substituting chemical coagulants with natural ones may reduce sludge handling costs. The use of conventional coagulants generates a massive volume of non-biodegradable sludge. This sludge is often disposed of in conventional landfills, as there is currently no rule tightly regulating the management of aluminum and iron in sludge. It has been demonstrated that the use of biocoagulants/biofloculants significantly reduces the amount of sludge generated during treatment operations by up to 30% (Kurniawan et al., 2020). Additionally, since all *Pinus halepensis* byproducts are biodegradable organics, the sludge may be utilized as a fertilizer as long as no heavy metals are present in the treated water. The present findings demonstrate the great efficiency of PhsEXT as a natural coagulant substitute for traditional ones.

Table 6 Comparison of *Pinus halepensis* Mill. seeds based biocoagulant with ferric chloride (FeCl_3) in coagulating Congo red. (Mean \pm SD, n = 3)

Coagulant	Coagulant dosage (mL L ⁻¹)	% Dye removal	Sludge volume (mL L ⁻¹)
PhsEXT	10	81.2 \pm 3.7	28 \pm 1
FeCl₃	10	83.8 \pm 3.6	46 \pm 1

4. Conclusion

The findings of the current investigation show that PhsEXT has significant potential as a natural coagulant and may thus be considered an interesting contribution in the field of natural resources development. At pH = 3, optimum performance was achieved with a biocoagulant dosage of 10 mL L⁻¹ and an initial Congo red concentration of 50 mg L⁻¹, yielding 81% of dye removal. Under acidic conditions, PhsEXT performed similarly to ferric chloride, yet produced less sludge and larger flocs. Seed's proximate composition and FTIR analysis corroborate the theory that charge neutralization (proteins— SO_3^{2-} groups of the dye) is the main mechanism occurring in this study. Due to the very high statistical coefficients ($R = 0.9998$, $R^2 = 0.9995$, and $R^2 \text{ adj} = 0.9995$)

and significantly lower statistical errors (RMSE = 0.5813, MSE = 0.3379, EPM = 0.9808, ESP = 0.9677, and MAE = 0.2382), the SVM_GWO model exhibited remarkable accuracy. In addition, the efficacy of the model was demonstrated using a variety of methodologies, including test interpolation and residual analysis. This highlights the advantages of combining SVM with GWO.

The outcomes of this work indicate that *Pinus halepensis* seeds as a biocoagulant has a promising future in the wastewater treatment field and may be a good alternative to chemical coagulants/flocculants in order to reduce environmental pollution and health hazards associated with their usage.

Acknowledgements

The authors would like to thank everyone who assisted them with this project.

Funding

The study is not dependent on any particular funding source in any form.

Compliance with Ethical Standards

The submitted work is an original article. It does not contain any human/animal experiments. The paper is original, has not been submitted to another journal for simultaneous review, and has not been published in any form or language elsewhere.

Data availability statement

The authors certify that the data backing the study's conclusions are included in the publication [and/or] its supplemental materials.

Competing interests

The authors state that they do not have any conflicting interests.

References

- Abidin, Z.Z., Ismail, N., Yunus, R., Ahamad, I., Idris, A., 2011. A preliminary study on *Jatropha curcas* as coagulant in wastewater treatment. *Environ. Technol.* 32, 971–977.
- Adenan, N.H., Lim, Y., Ting, A., 2022. Removal of triphenylmethane dyes by *Streptomyces bacillaris*: A study on decolorization, enzymatic reactions and toxicity of treated dye solutions. *J. Environ. Manage.* 318, 115520. <https://doi.org/10.1016/j.jenvman.2022.115520>
- Adnan, O., Abidin, Z.Z., Idris, A., Kamarudin, S., Al-Qubaisi, M.S., 2017. A novel biocoagulant agent from mushroom chitosan as water and wastewater therapy. *Environ. Sci. Pollut. Res.* 24, 20104–20112.
- Ali, S.S., Al-Tohamy, R., Mahmoud, Y.A.-G., Kornaros, M., Sun, S., Sun, J., 2022. Recent advances in the life cycle assessment of biodiesel production linked to azo dye degradation using yeast symbionts of termite guts: A critical review. *Energy Rep.* 8, 7557–7581.
- Al-Ismail, K., Al-Assoly, N., Saleh, M., 2018. Extraction and functional characterization of isolated proteins from Aleppo pine seeds (*Pinus halepensis* Mill.). *J. Food Meas. Charact.* 12, 386–394.
- Alnawajha, M.M., Kurniawan, S.B., Imron, M.F., Abdullah, S.R.S., Hasan, H.A., Othman, A.R., 2022. Plant-based coagulants/flocculants: characteristics, mechanisms, and possible utilization in treating aquaculture effluent and benefiting from the recovered nutrients. *Environ. Sci. Pollut. Res.* 1–24.
- Amran, A.H., Zaidi, N.S., Syafiuddin, A., Zhan, L.Z., Bahrodin, M.B., Mehmood, M.A., Boopathy, R., 2021. Potential of carica papaya seed-derived bio-coagulant to remove turbidity from polluted water assessed through experimental and modeling-based study. *Appl. Sci.* 11, 5715.
- Araújo, B., Romao, L., Doumer, M., Mangrich, A., 2016. Evaluation of the interactions between chitosan and humics in media for the controlled release of nitrogen fertilizer. *J. Environ. Manage.* 190, 122–131. <https://doi.org/10.1016/j.jenvman.2016.12.059>
- Ávila, C., Cañas, R.A., de la Torre, F.N., Pascual, M.B., Castro-Rodríguez, V., Cantón, F.R., Cánovas, F.M., 2022. Functional Genomics of Mediterranean Pines, in: *The Pine Genomes*. Springer, pp. 193–218.
- Aziz, H.A., Ramli, S.F., 2017. Settling velocity of sludge in coagulation flocculation treatment of leachate using ferric chloride and chitosan. Presented at the AIP Conference Proceedings, AIP Publishing LLC, p. 040028.
- Bahrodin, M.B., Zaidi, N.S., Hussein, N., Sillanpää, M., Prasetyo, D.D., Syafiuddin, A., 2021. Recent advances on coagulation-based treatment of wastewater: transition from chemical to natural coagulant. *Curr. Pollut. Rep.* 7, 379–391.

722 Baptista, A.T.A., Silva, M.O., Gomes, R.G., Bergamasco, R., Vieira, M.F., Vieira,
 723 A.M.S., 2017. Protein fractionation of seeds of *Moringa oleifera* Lam and its application
 724 in superficial water treatment. *Sep. Purif. Technol.* 180, 114–124.

725 Bargagli Stoffi, F.J., Cevolani, G., Gnecco, G., 2022. Simple Models in Complex
 726 Worlds: Occam's Razor and Statistical Learning Theory. *Minds Mach.* 32, 13–42.

727 Bello-Rodríguez, V., Cubas, J., Fernández, Á.B., Aguilar, M.J.D.A., González-
 728 Mancebo, J.M., 2020. Expansion dynamics of introduced *Pinus halepensis* Miller
 729 plantations in an oceanic island (La Gomera, Canary Islands). *For. Ecol. Manag.* 474,
 730 118374.

731 Beltrán, J., Sánchez-Martín, J., Delgado-Regalado, A., 2009. Removal of Carmine
 732 Indigo Dye with *Moringa oleifera* Seed Extract. *Ind. Eng. Chem. Res.* 48, 6512–6520.
 733 <https://doi.org/10.1021/ie9004833>

734 Benimam, H., Si-Moussa, C., Laidi, M., Hanini, S., 2020. Modeling the activity
 735 coefficient at infinite dilution of water in ionic liquids using artificial neural networks and
 736 support vector machines. *Neural Comput. Appl.* 32. [https://doi.org/10.1007/s00521-](https://doi.org/10.1007/s00521-019-04356-w)
 737 019-04356-w

738 Bouchelkia, N., Tahraoui, H., Amrane, A., Belkacemi, H., Bollinger, J.-C., Bouzaza, A.,
 739 Zoukel, A., Zhang, J., Mouni, L., 2022. Jujube stones based highly efficient activated
 740 carbon for methylene blue adsorption: kinetics and isotherms modeling,
 741 thermodynamics and mechanism study, optimization via Response surface
 742 methodology and machine learning approaches. *Process Saf. Environ. Prot.* 170, 513–
 743 535. <https://doi.org/10.1016/j.psep.2022.12.028>

744 Bousselma, A., Abdessemed, D., Tahraoui, H., Amrane, A., 2021. Artificial intelligence
 745 and mathematical modelling of the drying kinetics of pre-treated whole apricots. *Kem.*
 746 *U Ind.* 70, 651–667.

747 Chethana, M., Sorokhaibam, L.G., Bhandari, V.M., Raja, S., Ranade, V.V., 2016.
 748 Green approach to dye wastewater treatment using biocoagulants. *ACS Sustain.*
 749 *Chem. Eng.* 4, 2495–2507.

750 Chua, S.-C., Malek, M.A., Chong, F.-K., Sujarwo, W., Ho, Y.-C., 2019. Red lentil (*Lens*
 751 *culinaris*) extract as a novel natural coagulant for turbidity reduction: An evaluation,
 752 characterization and performance optimization study. *Water* 11, 1686.

753 Colombo, M., 2017. Regularity results for very degenerate elliptic equations, in: *Flows*
 754 *of Non-Smooth Vector Fields and Degenerate Elliptic Equations*. Springer, pp. 119–
 755 157.

756 Crini, G., Torri, G., Lichtfouse, E., Kyzas, G.Z., Wilson, L.D., Morin-Crini, N., 2019. Dye
 757 removal by biosorption using cross-linked chitosan-based hydrogels. *Environ. Chem.*
 758 *Lett.* 17, 1645–1666.

759 Dalvand, A., Gholibegloo, E., Ganjali, M.R., Golchinpoor, N., Khazaei, M., Kamani, H.,
 760 Hosseini, S.S., Mahvi, A.H., 2016. Comparison of *Moringa stenopetala* seed extract as
 761 a clean coagulant with Alum and *Moringa stenopetala*-Alum hybrid coagulant to

762 remove direct dye from Textile Wastewater. *Environ. Sci. Pollut. Res.* 23, 16396–
 763 16405.

764 Dasgupta, J., Sikder, J., Chakraborty, S., Curcio, S., Drioli, E., 2015. Remediation of
 765 textile effluents by membrane based treatment techniques: a state of the art review. *J.*
 766 *Environ. Manage.* 147, 55–72.

767 Daverey, A., Tiwari, N., Dutta, K., 2019. Utilization of extracts of *Musa paradisica*
 768 (banana) peels and *Dolichos lablab* (Indian bean) seeds as low-cost natural coagulants
 769 for turbidity removal from water. *Environ. Sci. Pollut. Res.* 26, 34177–34183.

770 Domínguez, J.R., Beltrán de Heredia, J., González, T., Sanchez-Lavado, F., 2005.
 771 Evaluation of ferric chloride as a coagulant for cork processing wastewaters. Influence
 772 of the operating conditions on the removal of organic matter and settleability
 773 parameters. *Ind. Eng. Chem. Res.* 44, 6539–6548.

774 Dziędziński, M., Kobus-Cisowska, J., Stachowiak, B., 2021. *Pinus* species as
 775 prospective reserves of bioactive compounds with potential use in functional food—
 776 Current state of knowledge. *Plants* 10, 1306.

777 El-Din, G., Amer, A., Malsh, G., Hussein, M., 2017. Study on the use of banana peels
 778 for oil spill removal. *Alex. Eng. J.* 57. <https://doi.org/10.1016/j.aej.2017.05.020>

779 Ghodke, P., Sharma, A., Pandey, J., Chen, W.-H., Patel, A., Veeramuthu, A., 2021.
 780 Pyrolysis of sewage sludge for sustainable biofuels and value-added biochar
 781 production. *J. Environ. Manage.* 298, 113450.
 782 <https://doi.org/10.1016/j.jenvman.2021.113450>

783 Hadadi, A., Imessaoudene, A., Bollinger, J.-C., Assadi, A.A., Amrane, A., Mouni, L.,
 784 2022a. Comparison of Four Plant-Based Bio-Coagulants Performances against Alum
 785 and Ferric Chloride in the Turbidity Improvement of Bentonite Synthetic Water. *Water*
 786 14, 3324.

787 Hadadi, A., Imessaoudene, A., Bollinger, J.-C., Cheikh, S., Assadi, A.A., Amrane, A.,
 788 Kebir, M., Mouni, L., 2022b. Parametrical Study for the Effective Removal of Mordant
 789 Black 11 from Synthetic Solutions: *Moringa oleifera* Seeds' Extracts Versus Alum.
 790 *Water* 14, 4109. <https://doi.org/10.3390/w14244109>

791 Han, G., Du, Y., Huang, Y., Wang, W., Su, S., Liu, B., 2022. Study on the removal of
 792 hazardous Congo red from aqueous solutions by chelation flocculation and
 793 precipitation flotation process. *Chemosphere* 289, 133109.

794 Hussain, G., Haydar, S., 2019. Exploring potential of pearl millet (*Pennisetum*
 795 *glaucum*) and black-eyed pea (*Vigna unguiculata* subsp. *unguiculata*) as bio-
 796 coagulants for water treatment. *Desalination Water Treat* 143, 184–191.

797 Imessaoudene, A., Cheikh, S., Bollinger, J.-C., Belkhiri, L., Tiri, A., Bouzaza, A., El
 798 Jery, A., Assadi, A., Amrane, A., Mouni, L., 2022. Zeolite Waste Characterization and
 799 Use as Low-Cost, Ecofriendly, and Sustainable Material for Malachite Green and
 800 Methylene Blue Dyes Removal: Box–Behnken Design, Kinetics, and Thermodynamics.
 801 *Appl. Sci.* 12, 7587. <https://doi.org/10.3390/app12157587>

802 Kapse, G., Samadder, S., 2021. Moringa oleifera seed defatted press cake based
 803 biocoagulant for the treatment of coal beneficiation plant effluent. J. Environ. Manage.
 804 296, 113202.

805 Katheresan, V., Kansedo, J., Lau, S.Y., 2018. Efficiency of various recent wastewater
 806 dye removal methods: A review. J. Environ. Chem. Eng. 6, 4676–4697.

807 Kielkopf, C.L., Bauer, W., Urbatsch, I.L., 2020. Bradford assay for determining protein
 808 concentration. Cold Spring Harb. Protoc. 2020, pdb. prot102269.

809 Kristianto, H., Rahman, H., Prasetyo, S., Sugih, A.K., 2019. Removal of Congo red
 810 aqueous solution using Leucaena leucocephala seed's extract as natural coagulant.
 811 Appl. Water Sci. 9, 1–7.

812 Kristianto, H., Verren, L., Prasetyo, S., Sugih, A.K., 2021. Comparison of FeCl₃ and
 813 leucaena seeds FeCl₃ extract coagulation performance to treat synthetic Congo red
 814 wastewater. Presented at the AIP Conf. Proc., AIP Publishing LLC, p. 040003.
 815 <https://doi.org/10.1063/5.0062181>

816 Lapointe, M., Barbeau, B., 2017. Dual starch–polyacrylamide polymer system for
 817 improved flocculation. Water Res. 124, 202–209.

818 Liu, Y., Li, C., Bao, J., Wang, X., Yu, W., Shao, L., 2022. Degradation of azo dyes with
 819 different functional groups in simulated wastewater by electrocoagulation. Water 14,
 820 123.

821 Madrona, G.S., Serpelloni, G.B., Salcedo Vieira, A.M., Nishi, L., Cardoso, K.C.,
 822 Bergamasco, R., 2010. Study of the effect of saline solution on the extraction of the
 823 Moringa oleifera seed's active component for water treatment. Water. Air. Soil Pollut.
 824 211, 409–415.

825 Manholer, D.D., de Souza, M.T.F., Ambrosio, E., Freitas, T.K.F. de S., Geraldino,
 826 H.C.L., Garcia, J.C., 2019. Coagulation/flocculation of textile effluent using a natural
 827 coagulant extracted from Dillenia indica. Water Sci. Technol. 80, 979–988.

828 Megersa, M., Gach, W., Beyene, A., Ambelu, A., Triest, L., 2019. Effect of salt solutions
 829 on coagulation performance of Moringa stenopetala and Maerua subcordata for turbid
 830 water treatment. Sep. Purif. Technol. 221, 319–324.

831 Mirjalili, S., Mirjalili, S.M., Lewis, A., 2014. Grey Wolf Optimizer. Adv. Eng. Softw. 69,
 832 46–61. <https://doi.org/10.1016/j.advengsoft.2013.12.007>

833 Mishra, A., Yadav, A., Agarwal, M., Rajani, S., 2004. Polyacrylonitrile-grafted Plantago
 834 psyllium mucilage for the removal of suspended and dissolved solids from tannery
 835 effluent. Colloid Polym. Sci. 282, 300–303.

836 Momeni, M., Kahforoushan, D., Abbasi, F., Ghanbarian, S., 2018. Using
 837 Chitosan/CHPATC as coagulant to remove color and turbidity of industrial wastewater:
 838 Optimization through RSM design. J. Environ. Manage. 211, 347–355.
 839 <https://doi.org/10.1016/j.jenvman.2018.01.031>

840 Mouni, L., Belkhiri, L., Bollinger, J.-C., Bouzaza, A., Assadi, A., Tirri, A., Dahmoune,
841 F., Madani, K., Remini, H., 2018. Removal of Methylene Blue from aqueous solutions
842 by adsorption on Kaolin: Kinetic and equilibrium studies. *Appl. Clay Sci.* 153, 38–45.

843 Muniyasamy, A., Sivaporul, G., Gopinath, A., Lakshmanan, R., Altaee, A., Achary, A.,
844 Chellam, P.V., 2020. Process development for the degradation of textile azo dyes
845 (mono-, di-, poly-) by advanced oxidation process-Ozonation: Experimental & partial
846 derivative modelling approach. *J. Environ. Manage.* 265, 110397.
847 <https://doi.org/10.1016/j.jenvman.2020.110397>

848 Nhut, H., Hung, N., Lap, B., Han, L., Tri, T., Bang, N., Hiep, N., Ky, N., 2021. Use of
849 *Moringa oleifera* seeds powder as bio-coagulants for the surface water treatment. *Int.*
850 *J. Environ. Sci. Technol.* 18, 2173–2180.

851 Pan, J.R., Huang, C., Chen, S., Chung, Y.-C., 1999. Evaluation of a modified chitosan
852 biopolymer for coagulation of colloidal particles. *Colloids Surf. Physicochem. Eng. Asp.*
853 147, 359–364.

854 Pardede, A., Budihardjo, M., Purwono, 2018. The Removal of Turbidity and TSS of the
855 Domestic Wastewater by Coagulation-Flocculation Process Involving Oyster
856 Mushroom as Biocoagulant. *E3S Web Conf.* 31, 05007.
857 <https://doi.org/10.1051/e3sconf/20183105007>

858 Pritchard, M., Craven, T., Mkandawire, T., Edmondson, A., O'Neill, J., 2010. A study of
859 the parameters affecting the effectiveness of *Moringa oleifera* in drinking water
860 purification. *Phys. Chem. Earth Parts ABC* 35, 791–797.

861 Putra, R., Amri, R., Ayu, M., 2020. Turbidity removal of synthetic wastewater using
862 biocoagulants based on protein and tannin. Presented at the AIP Conference
863 Proceedings, AIP Publishing LLC, p. 040028.

864 Radhika, B., Aruna, K., 2022. ELUCIDATING A PATHWAY FOR DEGRADATION OF
865 AZO DYE REACTIVE RED 120 BY BACTERIAL CONSORTIUM. *J. Appl. Biol. Sci.* 16,
866 396–417.

867 Rodrigues, C.S., Madeira, L.M., Boaventura, R.A., 2013. Treatment of textile dye
868 wastewaters using ferrous sulphate in a chemical coagulation/flocculation process.
869 *Environ. Technol.* 34, 719–729.

870 Saldarriaga-Hernández, S., Melchor-Martínez, E., Carrillo Nieves, D., Parra, R., Iqbal,
871 H., 2021. Seasonal characterization and quantification of biomolecules from
872 sargassum collected from Mexican Caribbean coast – A preliminary study as a step
873 forward to blue economy. *J. Environ. Manage.* 298, 113507.
874 <https://doi.org/10.1016/j.jenvman.2021.113507>

875 Shamsnejati, S., Chaibakhsh, N., Pendashteh, A.R., Hayeripour, S., 2015.
876 Mucilaginous seed of *Ocimum basilicum* as a natural coagulant for textile wastewater
877 treatment. *Ind. Crops Prod.* 69, 40–47. <https://doi.org/10.1016/j.indcrop.2015.01.045>

878 Sun, Y., Li, D., Lu, X., Sheng, J., Zheng, X., Xiao, X., 2021. Flocculation of combined
879 contaminants of dye and heavy metal by nano-chitosan flocculants. *J. Environ.*
880 *Manage.* 299, 113589. <https://doi.org/10.1016/j.jenvman.2021.113589>

881 Šuvalija, S., Serdarević, A., Džubur, A., Lazović, N., 2022. Biocoagulants and
 882 Biofloculants in Water and Wastewater Treatment Technology. Presented at the
 883 International Conference “New Technologies, Development and Applications,”
 884 Springer, pp. 882–889.

885 Suykens, J., Van Gestel, T., De Brabanter, J., De Moor, B., Vandewalle, J., 2002. Least
 886 squares support vector machines, World Scientific Publishing, Singapore.

887 Szygula, A., Guibal, E., Palacín, M., Ruiz, M., Sastre, A., 2009. Removal of an anionic
 888 dye (Acid Blue 92) by coagulation–flocculation using chitosan. *J. Environ. Manage.* 90,
 889 2979–86. <https://doi.org/10.1016/j.jenvman.2009.04.002>

890 Tahraoui, H., Amrane, A., Belhadj, A.-E., Zhang, J., 2022a. Modeling the organic
 891 matter of water using the decision tree coupled with bootstrap aggregated and least-
 892 squares boosting. *Environ. Technol. Innov.* 27, 102419.
 893 <https://doi.org/10.1016/j.eti.2022.102419>

894 Tahraoui, H., Belhadj, A.-E., Amrane, A., Houssein, E.H., 2022b. Predicting the
 895 concentration of sulfate using machine learning methods. *Earth Sci. Inform.* 1–22.

896 Tahraoui, H., Belhadj, A.-E., Hamitouche, A., 2020. Prediction of the Bicarbonate
 897 Amount in Drinking Water in the Region of Médéa Using Artificial Neural Network
 898 ModellingPredviđanje količine bikarbonata u pitkoj vodi regije Médéa modeliranjem
 899 umjetnom neuronskom mrežom. *Kem. U Ind.* 69, 595–602.
 900 <https://doi.org/10.15255/KUI.2020.002>

901 Tahraoui, H., Belhadj, A.-E., Hamitouche, A., Bouhedda, M., Amrane, A., 2021a.
 902 Predicting the concentration of sulfate (SO₄²⁻) in drinking water using artificial neural
 903 networks: a case study: Médéa-Algeria. *DESALINATION WATER Treat.* 217.
 904 <https://doi.org/10.5004/dwt.2021.26813>

905 Tahraoui, H., Belhadj, A.-E., Moula, N., Bouranene, S., Amrane, A., 2021b.
 906 Optimisation and prediction of the coagulant dose for the elimination of organic
 907 micropollutants based on turbidity. *Kem. U Ind.* 70, 675–691.

908 Tahraoui, H., Belhadj, A.-E., Triki, Z., Boudella, N., Seder, S., Amrane, A., Zhang, J.,
 909 Moula, N., Tifoura, A., Ferhat, R., Bousselma, A., Mihoubi, N., 2022c. Mixed
 910 Coagulant-flocculant Optimization for Pharmaceutical Effluent Pretreatment Using
 911 Response Surface Methodology and Gaussian Process Regression. *Process Saf.*
 912 *Environ. Prot.* 169. <https://doi.org/10.1016/j.psep.2022.11.045>

913 Teh, C.Y., Wu, T.Y., Juan, J.C., 2014. Potential use of rice starch in coagulation–
 914 flocculation process of agro-industrial wastewater: treatment performance and flocs
 915 characterization. *Ecol. Eng.* 71, 509–519.

916 Tie, J., Jiang, M., Li, H., Zhang, S., Zhang, X., 2015a. A comparison between *Moringa*
 917 *oleifera* seed presscake extract and polyaluminum chloride in the removal of direct
 918 black 19 from synthetic wastewater. *Ind. Crops Prod.* 74, 530–534.

919 Tie, J., Li, P., Xu, Z., Zhou, Y., Li, C., Zhang, X., 2015b. Removal of Congo red from
 920 aqueous solution using *Moringa oleifera* seed cake as natural coagulant. *Desalination*
 921 *Water Treat.* 54, 2817–2824.

- Tukan, S., Al-Ismael, K., Ajo, R., Al-Dabbas, M., 2013. Seeds and seed oil compositions of Aleppo pine (*Pinus halepensis* Mill.) grown in Jordan. *Riv Ital Delle Sostanze Grasse* 90, 87–93.
- Vapnik, V., Golowich, S., Smola, A., 1996. Support vector method for function approximation, regression estimation and signal processing. *Adv. Neural Inf. Process. Syst.* 9.
- Vicente, C., Silva, J.R., Santos, A.D., Quinta-Ferreira, R.M., Castro, L.M., 2022. Combined Electrocoagulation and Physicochemical Treatment of Cork Boiling Wastewater. *Sustainability* 14, 3727.
- Vijayaraghavan, G., Shanthakumar, S., 2015. Efficacy of *Moringa oleifera* and *Phaseolus vulgaris* (common bean) as coagulants for the removal of Congo red dye from aqueous solution. *J. Mater. Environ. Sci.* 6, 1672–1677.
- Wang, C., Li, G., Ali, I., Zhang, H., Tian, H., Lu, J., 2022. The Management of Energy Transformation through Laser Charging in WPT for 5G Application: Prediction Model of the In0. 3Ga0. 7As Solar Cell. *Wirel. Commun. Mob. Comput.* 2022.
- Zaidi, N.S., Ting, W., Loh, Z., Bahrodin, M., Awang, N., Kadier, A., 2022. Assessment and optimization of a natural coagulant (*Musa paradisiaca*) peels for domestic wastewater treatment. *Environ. Toxicol. Manag.* 2, 7–13. <https://doi.org/10.33086/etm.v2i1.2901>
- Zampeta, C., Bertaki, K., Triantaphyllidou, I.-E., Frontistis, Z., Vayenas, D., 2021. Treatment of real industrial-grade dye solutions and printing ink wastewater using a novel pilot-scale hydrodynamic cavitation reactor. *J. Environ. Manage.* 297, 113301. <https://doi.org/10.1016/j.jenvman.2021.113301>
- Zhang, X., Ye, P., Wu, Y., 2022. Enhanced technology for sewage sludge advanced dewatering from an engineering practice perspective: A review. *J. Environ. Manage.* 321, 115938.
- Zurina, A.Z., Mohd Fadzli, M., Abdul Ghani, L.A., 2014. Preliminary study of rambutan (*Nephelium lappaceum*) seed as potential biocoagulant for turbidity removal. Presented at the Advanced Materials Research, Trans Tech Publ, pp. 96–105.

Supplementary Materials

1. Influence of defatting *Pinus halepensis* Mill. seed on coagulation efficiency

the presence of oil might inhibit the extractability of protein and, ultimately, the efficacy of the coagulation process; this phenomenon has been described in a number of prior works (Camacho et al., 2017; Marobhe and Sabai, 2021; Yimer and Dame, 2021). In this regard, a preliminary investigation was conducted on the influence of delipidation on the Aleppo pine seeds coagulation efficiency for the removal of Congo red dye. A hexane extraction was performed according to the methodology given by (Chales et al., 2022). The oil extraction was conducted using a Soxhlet extractor equipment with hexane as the solvent and a solid/solvent ratio of 0.05 g/mL over a period of 3 h (20 cycles) to achieve a high oil-removal yield in comparison to other removal approaches (batch) or other solvents (ethanol, ethyl acetate, and acetone). The resulting defatted powder was subjected to the same extraction procedure depicted in the manuscript, 5 g were stirred vigorously with 100 mL of 1 M NaCl solution, the coagulation performance of crude and defatted seeds was then evaluated, and the results are presented in the following figure:

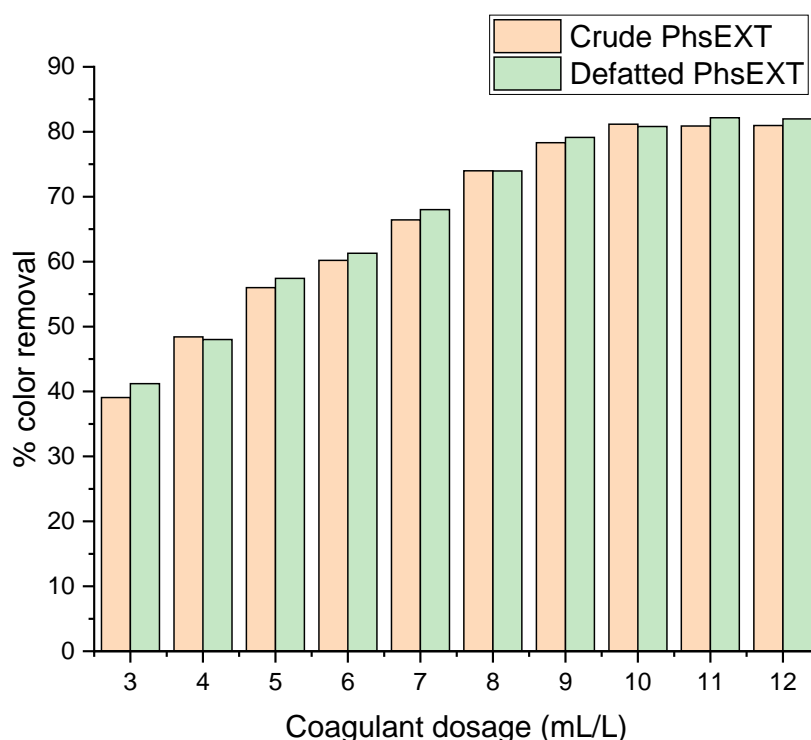


Fig. 1. Effect of coagulant dosage on the color removal efficiency of crude and defatted PhsEXT (pH = 3; [NaCl] = 1 M; T = 25°C)

979
980
981
982
983
984
985
986
987
988

989

990
991
992
993
994
995
996
997

998
999
1000
1001
1002
1003
1004
1005
1006
1007

1008

As shown in **Fig. 1**, there is a little variation in the removal efficiency of Congo red with seeds that have been defatted, suggesting that this step does not greatly enhance the process and might be skipped, especially because one of our primary objectives was to undertake the dye removal by the novel green coagulant with as few steps as possible to preserve the eco-friendly nature of the investigation. Such results have been reported by (Chales et al., 2022), indeed, the defatting step of *Moringa oleifera* seeds (MOS) did not improve the turbidity removal capacity of seeds' saline extract, but rather reduced the cytotoxicity of the treated water and generated a significant by-product (edible MOS oil).

2. *Pinus halepensis* Mill. seed extract (PhsEXT) coagulating agent

Concerning the possible influence of carbohydrates on the coagulation performance, a preliminary investigation was carried out in order to confirm or refute this possibility. Indeed, as is well known in the domain of biocoagulation-bioflocculation, natural coagulants are typically made up of carbohydrates and protein, with polysaccharide and amino acids functioning as the building blocks, either through charge neutralization, generally attributable to amino acids, or bridging phenomenon, usually linked to polysaccharide. The above mentioned phenomena are the primary mechanisms that govern biocoagulation-bioflocculation activity (Panwar et al., 2022).

A number of studies have reported the involvement of carbohydrates in the coagulation process (Mardarveran and Mohd Mokhtar, 2020) through the bridging mechanism. Our preliminary investigation involved examining the efficacy of an aqueous extract of Aleppo pine seeds according to the methodology reported in those previous studies. The dried *Pinus halepensis* seeds were sieved to a particle size of 0.5 mm. Then, 5 g of the dried raw materials was soaked in 100 ml of distilled water and stirred vigorously for 30 minutes. The obtained extract was centrifuged and filtered according to the same methodology depicted in the manuscript and tested on a 50 mg/L Congo red solution, the results are presented in **Fig. 2** (results for saline extract were incorporated for comparative purposes).

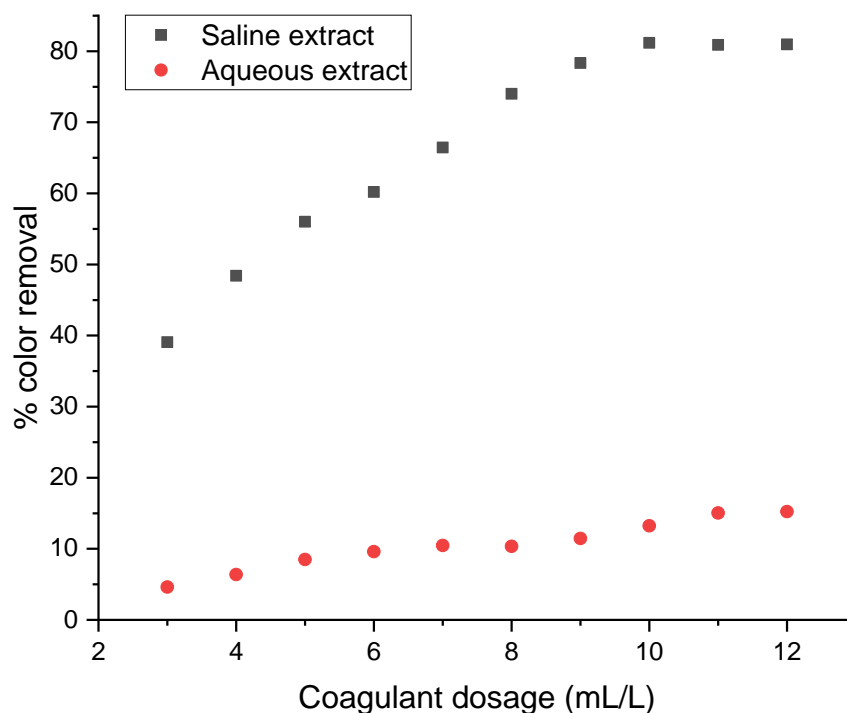


Fig. 2. Effect of coagulant dosage of saline and aqueous PHsEXT on the removal of Congo red (pH = 3; Congo red concentration = 50 mg/L; [NaCl] = 1 M; T = 25°C)

As can be observed in **Fig. 2**, there is a noticeable difference in the efficacy of the two seed extracts. The saline extract significantly outperforms the aqueous one, with an elimination rate of 80%, whereas the aqueous extract exhibits negligible Congo red removal. As stated in the manuscript, results and discussion section, (3.2.4. *Effect of NaCl concentration*), the increase in salt concentration promotes a better protein extraction through the salting-in mechanism, which refers to the process of increasing the ionic strength of a solution to boost solubility of protein leading, ultimately, to a dramatical increase in Congo red removal (from 0.1 M to 1 M NaCl).

Based on the data presented in **Fig. 2** and the section on the effect of NaCl concentration, it is obvious that proteins are the main protagonists in the coagulation process in this research.

This theory could also be confirmed by the effect of pH on coagulation efficiency (3.2.1. *Effect of initial pH on Congo red removal*), indeed, (Abidin et al., 2011; Bahrodin

et al., 2021) reported that the coagulation mechanism is charge neutralization when the difference between maximum removal and minimum removal by using different pH is around 50% or more, which is the case in our investigation. Also, bridging cannot be considered as a possible mechanism because unlike charge neutralization, bridging is least affected by pH. however, at lower pH, the polymeric chains responsible for interparticle bridging will expand and be able to attach to additional pollutants (Momeni et al., 2018; Zaidi et al., 2022).

3. Effect of slow stirring time and floc settling time on dye removal

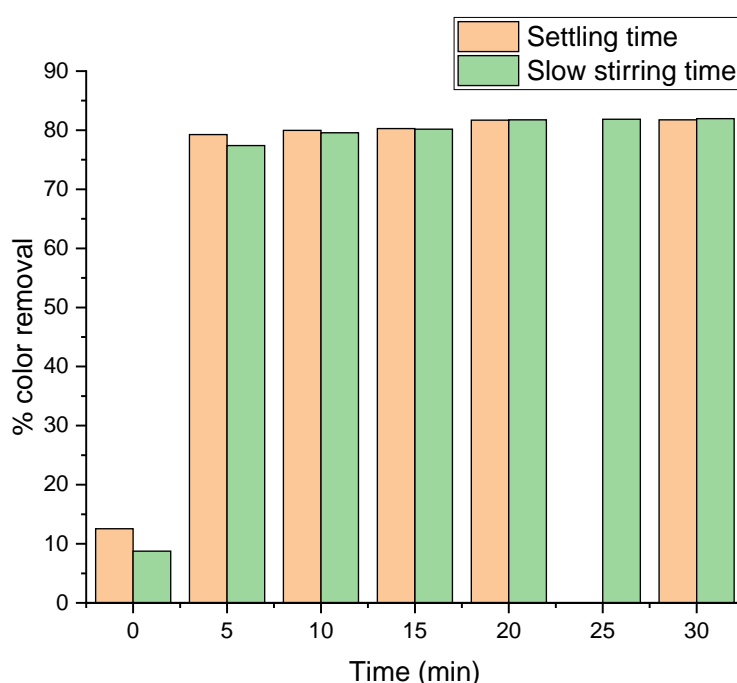


Fig. 3. Effect of stirring time (flocculation stage) and settling time on dye removal efficiency.

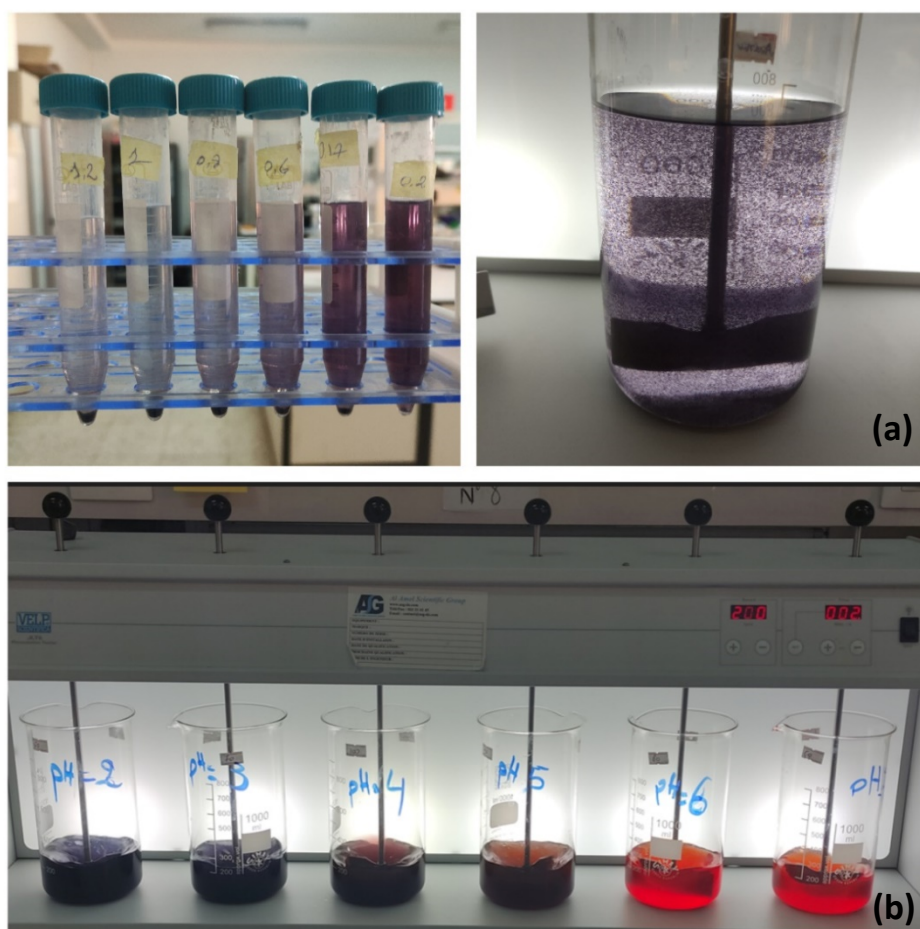


Fig. 4. (a) Representation of the discoloration process after treatment with *PhsEXT*,
(b) Jar-test apparatus used in this study.

4. Interface for optimization and prediction

To provide a simple way to implement the optimization and predict the removal rate of Congo red by biocoagulant, an interface was designed using the MATLAB guide for optimization and prediction (**Fig. 5**). This interface tool has been converted into an executable application under Windows. This powerful direct-to-use application predicts the output by selecting values input by SVM_GWO. In addition, the application also helps to find an optimal solution by GWO.

Application_for_prediction_and_optimization

Prediction and optimization using SVM_GWO model

Optimal optimization by GWO based on SVM_GWO model

Inputs	Parameter Range	
	Min	Max
Stirring time (min)	0	20
Sedimentation time (min)	0	30
Initial concentrat (mg/L)	50	50
Dosage (ml/L)	3	12
pH	1	12
NaCl Concentrat (M)	0.1	2
Stirring speed (rpm)	0	110
Temperature (°C)	10	60

Run

GWO

Prediction using SVM_GWO model

CLC: to Delete all values

Run

CLC

Optimal inputs

20
30
50
10
3
1
30
25

Output

The predicted removal rate of Congo red (%)

81.1746

(a)

Application_for_prediction_and_optimization

Prediction and optimization using SVM_GWO model

Optimal optimization by GWO based on SVM_GWO model

Inputs	Parameter Range	
	Min	Max
Stirring time (min)	0	20
Sedimentation time (min)	0	30
Initial concentrat (mg/L)	150	150
Dosage (ml/L)	3	12
pH	1	12
NaCl Concentrat (M)	0.1	2
Stirring speed (rpm)	0	110
Temperature (°C)	10	60

Run

GWO

Prediction using SVM_GWO model

CLC: to Delete all values

Run

CLC

Optimal inputs

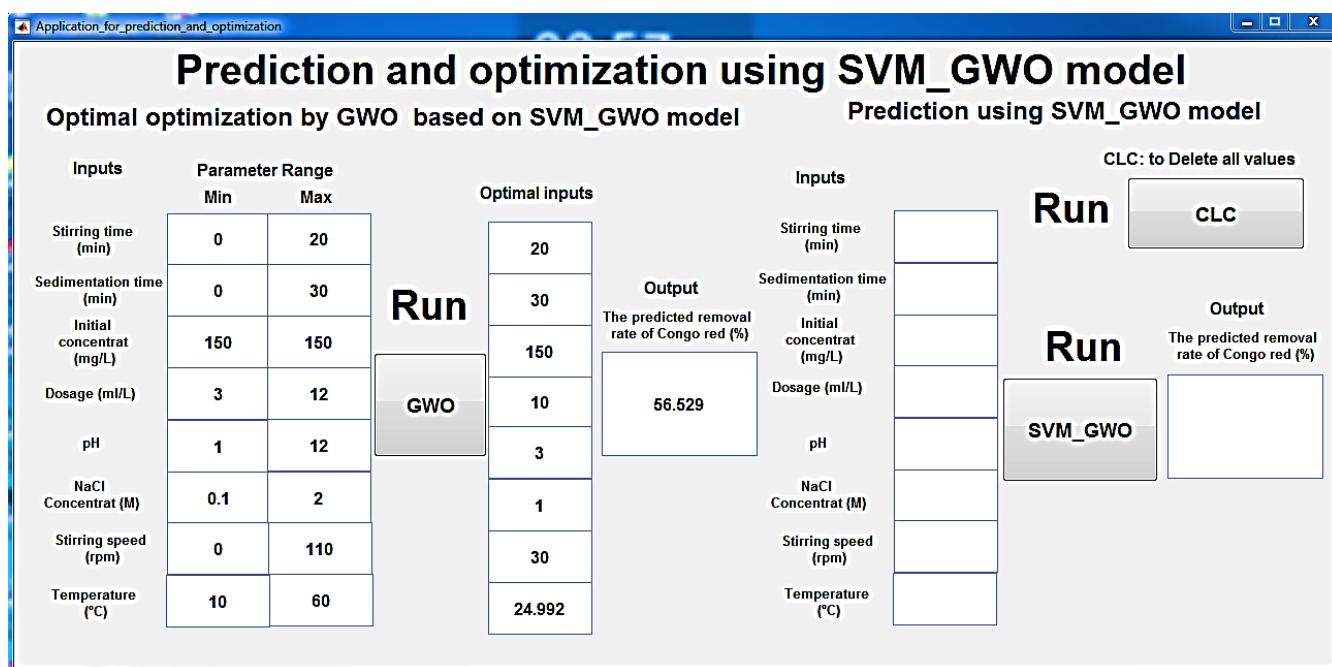
20
30
150
10
3
1
30
24.992

Output

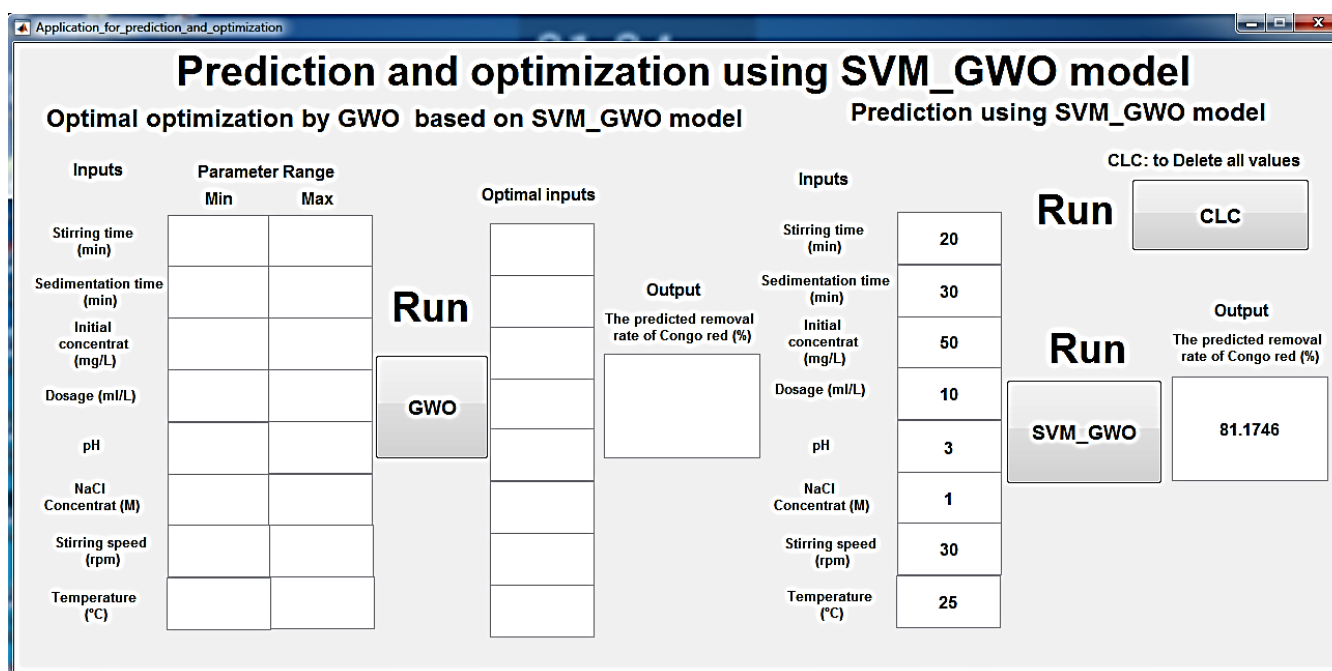
The predicted removal rate of Congo red (%)

56.529

(b)



(c)



(d)

Fig. 5. MATLAB Interface: Optimization of optimal using GWO for (a) concentration 50 mg/L, (b) concentration 150 mg/L, (c) concentration 170 mg/L, and (d) prediction the removal rate of Congo red with SVM_GWO model.

Supplementary Materials references

- Abidin, Z.Z., Ismail, N., Yunus, R., Ahamad, I., Idris, A., 2011. A preliminary study on *Jatropha curcas* as coagulant in wastewater treatment. *Environ. Technol.* 32, 971–977.
- Bahrodin, M.B., Zaidi, N.S., Hussein, N., Sillanpää, M., Prasetyo, D.D., Syafiuddin, A., 2021. Recent advances on coagulation-based treatment of wastewater: transition from chemical to natural coagulant. *Curr. Pollut. Rep.* 7, 379–391.
- Camacho, F., Serrão Sousa, V., Bergamasco, R., Teixeira, M., 2017. The use of *Moringa oleifera* as a natural coagulant in surface water treatment. *Chem. Eng. J.* 313, 226–237. <https://doi.org/10.1016/j.cej.2016.12.031>
- Chales, G., Tihameri, B., Vicensoto Moreira Milhan, N., Koga Ito, C., Antunes, M., Reis, A., 2022. Impact of *Moringa oleifera* Seed-Derived Coagulants Processing Steps on Physicochemical, Residual Organic, and Cytotoxicity Properties of Treated Water. *Water* 14, 2058. <https://doi.org/10.3390/w14132058>
- Mardarveran, P., Mohd Mokhtar, N., 2020. Performance of jackfruit (*Artocarpus heterophyllus*) peel coagulant in turbidity reduction under different pH of wastewater. *Mater. Today Proc.* 46. <https://doi.org/10.1016/j.matpr.2020.10.248>
- Marobhe, N., Sabai, S., 2021. Treatment of drinking water for rural households using *Moringa* seed and solar disinfection. *J. Water Sanit. Hyg. Dev.* 11. <https://doi.org/10.2166/washdev.2021.253>
- Momeni, M., Kahforoushan, D., Abbasi, F., Ghanbarian, S., 2018. Using Chitosan/CHPATC as coagulant to remove color and turbidity of industrial wastewater: Optimization through RSM design. *J. Environ. Manage.* 211, 347–355. <https://doi.org/10.1016/j.jenvman.2018.01.031>
- Panwar, K., Dadhich, I., Dave, M., Sharma, Y., Shaik, N., 2022. Effective Waste Water Treatment by the Application of Natural Coagulants. *Adv. Mater. Sci. Eng.* 2022, 1–5. <https://doi.org/10.1155/2022/3023200>
- Yimer, A., Dame, B., 2021. Papaya seed extract as coagulant for potable water treatment in the case of Tulte River for the community of Yekuset district, Ethiopia. *Environ. Chall.* 4, 100198. <https://doi.org/10.1016/j.envc.2021.100198>
- Zaidi, N.S., Ting, W., Loh, Z., Bahrodin, M., Awang, N., Kadier, A., 2022. Assessment and optimization of a natural coagulant (*Musa paradisiaca*) peels for domestic wastewater treatment. *Environ. Toxicol. Manag.* 2, 7–13. <https://doi.org/10.33086/etm.v2i1.2901>